

# Dynamic small-scale green ammonia non-renewable and renewable exergy costs up to 2050: Short and long-term projections under IEA energy transition scenarios

Alessandro Lima <sup>\*</sup>, Jorge Torrubia, César Torres, Alicia Valero, Antonio Valero

Research Institute for Energy and Resource Efficiency of Aragón (Institute ENERGAIA), University of Zaragoza, Edificio CIRCE, Calle Mariano Esquillor Gomez, 15, Zaragoza, 50018, Aragón, Spain

## ARTICLE INFO

### Keywords:

Green ammonia  
Green hydrogen  
Circular thermoeconomics  
Material intensity  
Renewable energies  
Energy transition

## ABSTRACT

Ammonia is currently indispensable for fertilizers and is projected to be a fundamental renewable energy vector. This study analyzes the non-renewable and renewable exergy costs associated with a small-scale green ammonia plant under different combinations of water electrolysis technologies (AWE, PEM, SOEC, and AEM) with electricity sources (hydro, wind, photovoltaic, and electricity grid). Our method accounts for both the exergy conversion efficiencies of primary energy sources and the required materials on the infrastructures of the renewables and electrolyzers. Our research projects current, short-term (2030) and long-term (2050) ammonia's exergy cost based on different IEA's energy transition scenarios. Our findings highlight the impact of non-renewable exergy consumption on the renewables and electrolyzers infrastructures on ammonia exergy costs. In 2025, these values range between 12.5 and 32.5 MWh/t<sub>NH<sub>3</sub></sub>, whereas in 2050 they might range between 11.5 and 19.1 MWh/t<sub>NH<sub>3</sub></sub> for SOEC-hydro and PEM-AWE-electricity grid scenarios, respectively. A Grassmann diagram illustrates how non-renewable and renewable exergy costs are split throughout the natural resources of our plant. A discussion about the model's main features, restrictions and future industrial symbiosis possibilities (Ar, H<sub>2</sub>, O<sub>2</sub>) is presented. Our innovative methodology emphasizes the origins of natural resources by conscientiously evaluating their non-renewable and renewable exergy costs.

## 1. Introduction

Ammonia has been fundamental for fertilizers and therefore for agriculture. Some estimations state that nearly 40% of the global human population depended on synthesized ammonia fertilizers for food [1]. Gray and blue ammonia production relies on natural gas and on the Haber-Bosch process. These industries are very energy-demanding with non-renewable natural gas and account for 2% (8.6EJ) of the global energy consumption. Consequently, they release around 451 Mt of carbon dioxide per year to produce 157 Mt of ammonia, thus resulting in a yearly average plant emission of t<sub>CO<sub>2</sub></sub>/t<sub>NH<sub>3</sub></sub>. On the other hand, estimations about ammonia production suggest an increase of 31% up to 2030 [2], and in 2050 we will likely need almost 688 Mt of ammonia to cover new demands, such as, shipping, hydrogen carrier, power generation, and the traditional fertilizers production [3].

Under this context, green ammonia has received huge attention over the last years as a solution for the non-sustainability issue [4]. Basically, green ammonia plants (GAP) consumes renewable hydrogen from water electrolysis or biomass instead of non-renewable natural gas. However,

GAPs have some primary economical issues that need to be addressed to their implementation. Self-sustenance, flexibility, low electric power cost, and minimization of supply chain costs and custom duties are some mandatory factors that need to be accounted for to achieve a low CAPEX, OPEX, and economic viability. Green ammonia' current prices are around 720 \$/t for the most adequate renewable energy locations, but projected scenarios for 2030 and 2050 suggest costs around 310–500\$/t<sub>NH<sub>3</sub></sub> [3,4] due to green hydrogen cost reduction.

The flexibility of green ammonia synthesis plants have received significant scientific attention recently [5], because it is more efficient and cost-effective to consume hydrogen locally [6]. GAP small-scale plants (10 000–15 000 t<sub>NH<sub>3</sub></sub>/y) will require operational flexibility for dynamic conditions due to intermittent weather behavior [7–10]. Also, these will likely involve green hydrogen production systems while mitigating transport, energy infrastructure, and storage costs for low CAPEX and minimum CO<sub>2</sub> emissions. All these features mentioned diverge from traditional configurations of gray or blue ammonia plants, which were optimized to operate based on the economy of scale. And

<sup>\*</sup> Corresponding author.

E-mail address: [atruta@unizar.es](mailto:atruta@unizar.es) (A. Lima).

<https://doi.org/10.1016/j.renene.2025.123891>

Received 31 January 2025; Received in revised form 2 May 2025; Accepted 28 June 2025

Available online 17 July 2025

0960-1481/© 2025 The Authors. Published by Elsevier Ltd. This is an open access article under the CC BY license (<http://creativecommons.org/licenses/by/4.0/>).

even though these plants are optimized and very energy efficient, they are not adequate for the current needs [11].

Under this context, four water electrolysis technologies, alkaline water electrolysis (AWE), proton exchange membrane (PEM) electrolysis, solid oxide electrolysis cells (SOECs), and anion exchange membrane (AEM) electrolysis, are included in our study. Their technology readiness levels (TRLs) significantly differ [12–14], making it fundamental to evaluate how they affect the overall exergy costs of green  $H_2$  and consequently green ammonia. AWE is a mature and commercial technology that features precious material independence in its construction and operation (Ni in electrodes and Zr in the separator), but its operation is not very flexible for intermittent renewable energy sources. PEM was first introduced in the 1960s by General Electric to overcome some AWE operational drawbacks. They offer a very flexible operation, but they require expensive electrodes (platinum group metals, PGMs), and is currently have a shorter lifetime than AWE [2]. SOEC and AEM are the most novel ones among the four and are still under R&D. SOEC use ceramics as electrolytes, have lower material costs, operate at higher temperatures and efficiencies [2]. Their structure currently uses Zr, La, Y, and Ni, thus also depends on critical metals to operate efficiently. On the other hand, AEM is freer from noble metals than PEM and adopts low-concentrated liquid electrolytes (1 M KOH) [13]. However, it currently presents limited stability and is still in research and development stages. In summary, all four electrolysis technologies present advantages and drawbacks [12–15] that affect the overall exergy costs of hydrogen and ammonia over the years, thus their efficiency and lifetime evolution up to 2050 require a proper analysis.

Exergy analyses of gray ammonia production systems are already well covered by specialized literature [16,17]. For green ammonia, there are some examples about different plant configurations available on the literature: Investigations about local techno-economic, thermoeconomic, and 4E assessments of green hydrogen and ammonia production systems have been gaining highlight recently [9,18–20]. These also involve steady-state and dynamic operations [7,21,22]. However, these all focused on higher-scale plants. Alternative studies on small-scale plant applications are also available [23,24], but we require further investigations to estimate the non-renewable and renewable exergy costs [25] of green ammonia.

This paper presents a projection of overall exergy costs range associated with a small-scale GAP under different combinations of water electrolysis technologies (AWE, PEM, SOEC, and AEM) and electricity sources (hydro, wind, PV, and electricity grid). We evaluated possible electricity and hydrogen production scenarios up to 2050 under IEA's projected energy transition scenarios: Net-Zero Emissions (NZE), Announced Pledges Case (APC), and Stated Policies (STEPS). The combined energy scenarios are fundamental to check how renewable these systems can be, and to properly realize green ammonia's exergy costs in our designed plant. Furthermore, we highlight the impact non-renewable and renewable exergy cost contributions of the plant's inputs and infrastructure (energy intensity and mineral exergy of materials) on the exergy costs of our GAP product. Also, we present an illustrative example of non-renewable and renewable exergy costs of green ammonia production via a Grassmann diagram. Finally, we discuss the model restrictions and expansions, and future studies based on the industrial symbiosis concept. It is expected that both the exergy costs of ammonia under the studied scenarios and presented discussion help elucidate the importance of small-scale plants to enhance their ecological footprint.

## 2. Methodology

The methodology is divided in the following subsections: Section 2.1 describes the mathematical model of our small-scale GAP and natural resources adopted in our study. Next, Section 2.2 summarizes the plant features, process flow diagram and model assumptions. Then, Section 2.3 discusses the ammonia plant modeling on Aspen Plus V14.0 and the software integration with MATLAB and TAES. Lastly, Section 2.4 discusses the dynamic evaluation of natural resources exergy costs related to our work.

### 2.1. Model description

Fig. 1 represents a simplified, yet expanded view of a small-scale GAP by integrating our synthesis plant with primary energy sources (PES), water electrolysis for hydrogen production, an air separation unit (ASU) for nitrogen production, tanks for storing both reactants, etc. For this work, the authors only included the systems colored in Fig. 1, that is, the PES unit, the water electrolyzers, the ASU, and the ammonia synthesis unit.

The inputs adopted in our model are mostly natural resources in order to reinforce the idea of checking the renewability of our GAP. We included material and energy intensities required by the infrastructures of each industrial unit taken into consideration. For example, in this study, we accounted the investments on materials, fossil fuels and electricity on the infrastructures of the PES [25,26] and water electrolyzers. These are the following:

- Water: groundwater for cooling water and electrolysis, and river water as renewable energy source for a hydroelectric plant (Hydro);
- Air: air separation unit (ASU) for nitrogen separation and for cooling;
- Sunlight: renewable energy source from a solar photovoltaic plant (PV);
- Wind: renewable energy source for a wind plant (Wind);
- Materials: required for the renewable energy systems and electrolysis infrastructure.

### 2.2. Plant features, process flow diagram, and model assumptions

In order to reach our described goals, the first step was to develop a mathematical model that allowed a circular thermoeconomic analysis of a representative green ammonia production process. Fig. 2 presents the process flow diagram (PFD) of the green ammonia synthesis plant developed in Aspen PLUS v14. This plant produces 10231.6 t/year of ammonia and Table A.2 summarizes the plant configuration in Appendix A. The ammonia synthesis reaction was modeled based on the kinetic data obtained from [27]. The compressor power and heat transfers are available on Table 1.

### 2.3. Green ammonia plant modeling, exergy and circular thermoeconomic analyses

Our chemical plant model was developed on Aspen PLUS and the thermodynamic properties were evaluated based on Soave-Redlich-Kwong Equation of State (SRK-BM EoS). The chemical exergy contribution was evaluated based on an in-house MATLAB code developed for real gases, by taking into account the activity coefficients and standard-state exergy under reference conditions - 298.15 K and 1 atmosphere [28]. Table A.3 in Appendix A presents the exergy flows of all streams involved and their molar composition. Temperature, pressure, and molar flows are available on Fig. 2. The exergy flow values  $\dot{B}$  are the main inputs of TAES (Thermoeconomic Analysis of Energy Systems), an in-house public (available in GitHub and in the Exergoecology Portal) software [29,30] built in MATLAB specialized in circular thermoeconomic analyses. Circular thermoeconomics combines the fundamentals of circular/spiral economy with the application of classical thermoeconomics and diagnostics of complex energy systems in order to evaluate the weights of natural resources exergy costs on the production of any industrial product. With estimations of all inputs, whether they are on physical (exergy cost,  $MWh/MWh_{input}$ ), economical (specific monetary cost,  $€/MWh_{input}$ ) and/or environmental ( $CO_2$  emissions,  $t_{CO_2}/MWh_{input}$ ) units, it is possible to project a cradle-to-gate analysis — but all in an exergetic basis. The revised Exergy Cost Theory (ECT) adopted in TAES includes fundamental aspects for circular economy, such as waste and recycle analyses, as well as process integration; all regardless of the system's productive structure complexity. The fuel-product equations adopted to our ammonia plant all unit operations are available on Table A.4 in Appendix A.

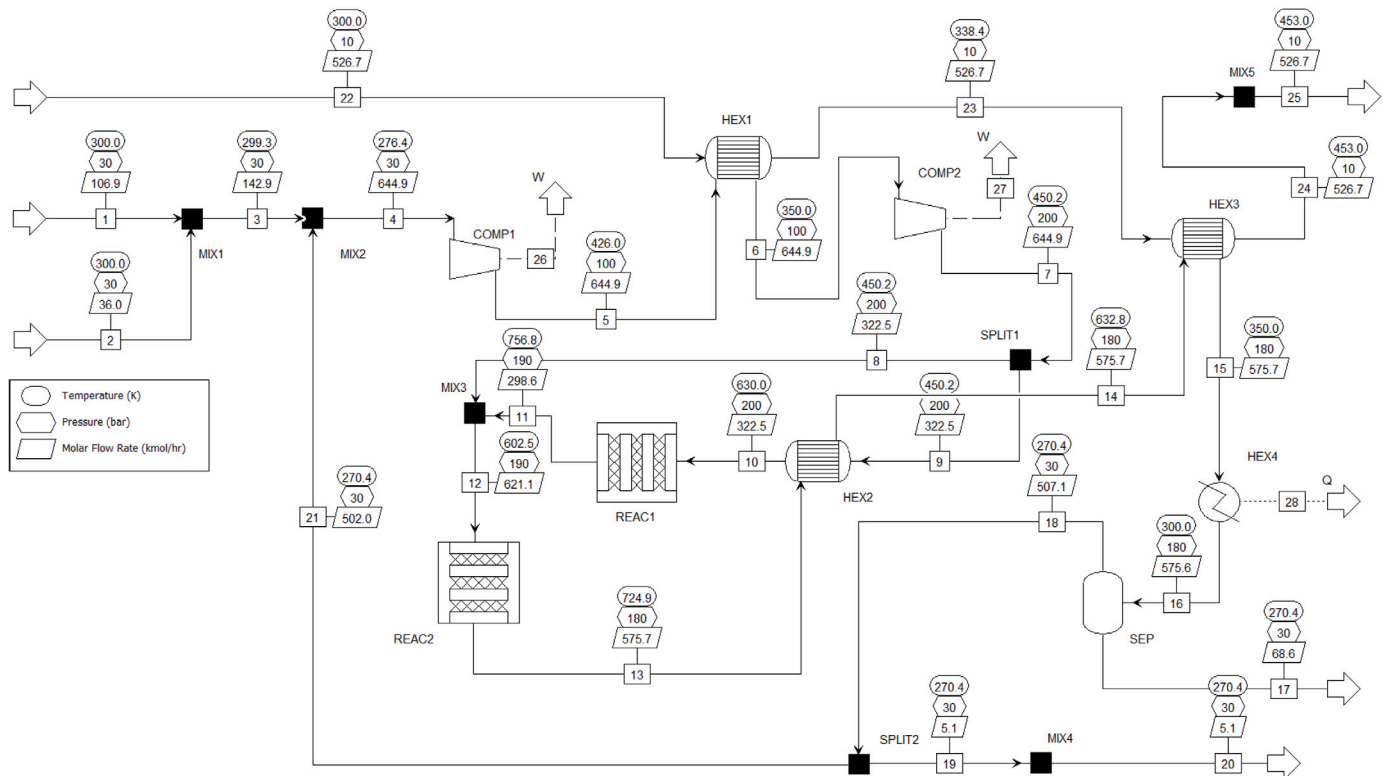
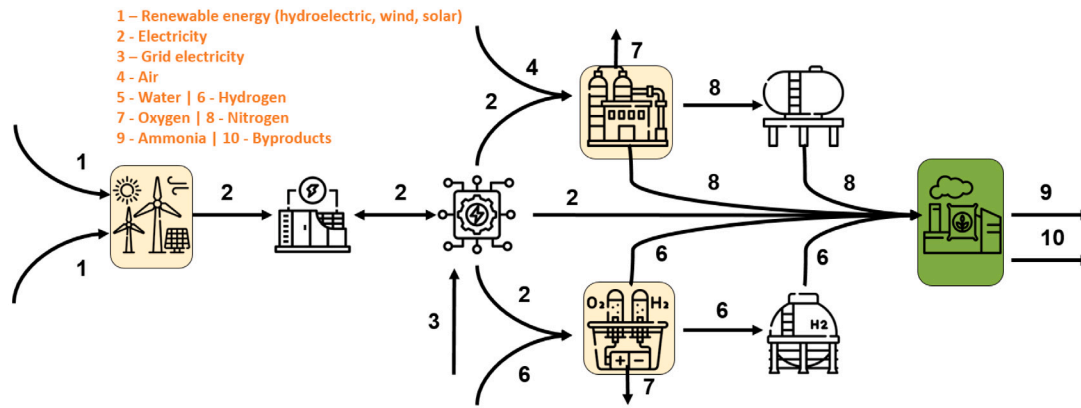


**Fig. 2.** Process flow diagram (PFD) of the green ammonia synthesis plant in study developed in Aspen Plus v14.

#### 2.4. Dynamic evaluation of natural resources exergy costs

The evaluation of the natural resources dynamic exergy costs is the following:

- Energy intensity and mineral exergy [15,31,32]. We accounted for the energy and material intensities (units in  $\text{kg}_{\text{mat}}/\text{MW}_{\text{el}}$ , and  $\text{MJ}_{\text{mat}}/\text{kg}_{\text{mat}}$ ) different materials between chemical species (e.g., Ag, Al, As, Au, B, Ba, Be, Cd, Ce, Co, Cr, Cu, Dy, Er, Eu, Fe, Ga, Gd, Hg, Ho, In, Ir, La, Li, Lu, Mg, Mn, Mo, Nb, Nd, Ni, Pb, Pd, Pr, Pt, Rh, Sb, Se, Si, Sm, Sn, Sr, Ta, Tb, Te, Ti, Tm, V, W, Y, Yb, Zn, Zr) and composite materials (e.g., stainless steel, concrete, plastic, glass, graphite) required on building the infrastructures of each PES and the water electrolyzer technologies.
- PES: For each technology, projection of electricity production installed capacity and demand: from 1900 to 2017 [26] and from

2023 to 2050 from IEA energy transition scenarios (NZE, APC, STATES) for required, installed, and decommissioned power [33], efficiency, lifespan, capacity factor, and EROI and EXROI [25,34];

- PES: Energy intensity, ExCOE and LExCOE [25];
- Water electrolyzer: For each technology, conversion efficiency, lifespan [2,12,35] and material intensities [14,15,32]. Hydrogen energy cost (process and infrastructure costs) was evaluated as [15,32].

The algorithm follows the modeling presented on previous works [15,31,32,34,36]. The unit exergy cost of each PES (or electrolyzer) is evaluated based on the energy conversion efficiency of each technology and on the energy footprints of required infrastructure materials (fossil fuels and electricity). Both the infrastructure and energy processes are evaluated in terms of each technology (i.e., natural gas, oil, coal, hydroelectric, nuclear, biomass, wind, and solar PV). The purpose

is to evaluate both the non-renewable (fossil fuels and nuclear) and renewable contributions of each technology. For example, the exergy costs for hydrogen involve the following equations [15]:

$$\bar{b}_{\text{Fuel,H}_2}^* = \frac{\bar{b}_{\text{PES,Electricity}}^*}{\bar{\eta}_{\text{Electrolyzer}}} \quad (1)$$

$$\begin{aligned} \bar{b}_{\text{Material,Electrolyzer}}^* &= M I_{\text{Material,Electrolyzer}}^* (\bar{b}_{\text{Material,FF}}^* + \bar{b}_{\text{Materials,Electricity}}^* \bar{b}_{\text{PES,Electricity}}^*) \quad (2) \end{aligned}$$

$$\bar{b}_{\text{Infra,Electrolyzer}}^* = \frac{\bar{b}_{\text{Material,Electrolyzer}}^*}{3600 t_{\text{Operation,Electrolyzer}}} \quad (3)$$

$$\bar{b}_{\text{H}_2}^* = \bar{b}_{\text{Fuel,H}_2}^* + \bar{b}_{\text{Infra,Electrolyzer}}^* \quad (4)$$

where  $\bar{b}_{\text{H}_2}^*$  is the  $\text{H}_2$ 's overall unit exergy cost vector  $\bar{b}_{\text{Fuel,H}_2}^*$  and  $\bar{b}_{\text{Infra,Electrolyzer}}^*$  represent its unit exergy costs of  $\text{H}_2$  production (i.e., electrolyzer energy conversion) and lifetime-averaged electrolyzer infrastructure manufacturing (i.e., energy consumed on materials extraction and refining),  $\bar{b}_{\text{PES,Electricity}}^*$  is the LExCOE vector for all PES,  $\bar{\eta}_{\text{Electrolyzer}}$  is the projected state-of-the-art electrolyzer efficiency for each year (Table B.6),  $\bar{b}_{\text{Materials,Electrolyzer}}^*$  corresponds to the energy intensity vector for all materials required by each electrolyzer manufacturing,  $M I_{\text{Material,Electrolyzer}}^*$  is the material intensity of each electrolyzer technology,  $\bar{b}_{\text{Material,FF}}^*$  and  $\bar{b}_{\text{Materials,Electricity}}^*$  represent the fossil fuels (natural gas, oil and coal) and electricity parts of the energy intensities of obtaining each required material, respectively, and  $t_{\text{Operation,Electrolyzer}}$  is the projected state-of-the-art electrolyzer lifetime for each year. A more detailed analysis applying this methodology to evaluate non-renewable and renewable  $\text{H}_2$  exergy costs is available on [15]. For the GAP case presented in this paper, we can estimate the ammonia unit exergy cost vector based on the evaluated  $\text{H}_2$ ,  $\text{N}_2$ ,  $\text{H}_2\text{O}$ , and electricity (LExCOE) exergy costs by Eq. (5):

$$\bar{b}_{\text{NH}_3}^* = \frac{\bar{B}_{\text{H}_2,1}^* + \bar{B}_{\text{N}_2,2}^* + \bar{B}_{\text{H}_2\text{O},22}^* + \sum_{i=1}^2 \bar{B}_{\text{Comp},i}^*}{B_{17}} \quad (5)$$

where  $\bar{b}_{\text{NH}_3}^*$  is the  $\text{NH}_3$  unit exergy cost,  $\bar{B}_{\text{H}_2,1}^*$ ,  $\bar{B}_{\text{N}_2,2}^*$ ,  $\bar{B}_{\text{H}_2\text{O},22}^*$ , and  $\bar{B}_{\text{Comp},i}^*$  correspond to the exergy cost vectors of the  $\text{H}_2$ ,  $\text{N}_2$ ,  $\text{H}_2\text{O}$ , and compressors streams on streams 1, 2, 22, 26, and 27, respectively. And  $B_{17}$  is the exergy flow of produced ammonia (stream 17).

Therefore, to proceed with the circular thermoeconomic analysis, first we need to discover appropriate values to represent the exergy costs of streams 1 (hydrogen), 2 (nitrogen + argon), 22 (water), 26, and 27 (compressors power) represented on Fig. 2. This approach allow us to evaluate the costs of our main product, stream 17 (liquid ammonia), and our wastes, streams 20, 25, and 28 (purge, water, and heat). The method applied to estimate these costs involves analyzing the origin of each input, as described next.

#### 2.4.1. Water exergy cost

To estimate the exergy costs of water used on the ammonia cooling process, we adopted the methodology described in [37] for water transfers and groundwater. Based on this methodology, we estimated the exergy cost of water transfers as 1.7917 kJ/kJ $_{\text{H}_2\text{O}}$ . This value is multiplied by the LExCOE of each year (Table B.8) to estimate the overall exergy cost for each IEA scenario.

#### 2.4.2. Electricity exergy cost

This work projects green ammonia exergy costs based on three distinct IEA energy transition scenarios for 2050: Net-Zero Emissions Scenario (NZE), Announced Pledges Case/Scenario (APC or APS), and Stated Policies Scenario (STEPS) [33,38]. These examine the consequences of possible energy transition pathways and the required scale

of the transformation based on all government energy and climate policies and pledges [38]. STEPS takes into account only specific policies that are in place or have been announced by governments. It provides a sense of our current direction of energy system progression, based on a detailed review of the current policies. APC goes forward and assumes that all net zero pledges are completely achieved on time and shows how far full implementation of these pledges would take the world towards reaching net-zero emissions. Lastly, NZE depicts a difficult but possible pathway for the global energy sector to reach net zero energy-related  $\text{CO}_2$  emissions by 2050 with a wide portfolio of clean energy technologies.

Naturally, these possible pathways come with uncertainties, especially those related to themes such as bioenergy, carbon capture and behavioral changes [38]. APC and STEPS diverges on the difference that current net zero pledges could make and highlight at the same time the need for concrete policies and short-term plans that are coherent with the goal. Table B.7 summarizes the electricity production (TWh and GW) and total  $\text{CO}_2$  emissions (Mt) for each IEA scenario. The energy transition requires substantial quantities of critical minerals (e.g., critical minerals like copper, cobalt, manganese, various rare earth metals, and so on), and their supply exponentially grows (seven-fold between 2020 and 2030 in the net zero pathway). This adequately fits with our goal of evaluating the weight of infrastructure costs on the proposed analysis.

Based on the latest available database from IEA [33] for these three scenarios, we projected the non-renewable and renewable leveled exergy cost of electricity (LExCOE) [25] to our analysis. Table B.8 presents the LExCOE for the renewable PES and the global grid electricity LExCOE adopted in this study under the three aforementioned scenarios between 2025 and 2050.

In this work, we evaluated the production of ammonia under 14 distinct electricity production pathways by assuming electricity production from either renewable energy sources (Hydro, wind, or solar PV) or electricity grid (grid) usage (Table B.8). Moreover, we projected alternatives where a hybridization of the consumed electricity exists between the renewable sources (e.g., hydro and wind, wind and solar PV, etc.) and also between renewable sources with the electricity grid (e.g., solar PV and grid, hydro, wind, and grid, etc.). In this hypothetical state, each source equally contributed to the electricity demand. For example, for a hydro and grid scenario, we assumed that our LExCOE is composed by 50% contribution from hydro and 50% contribution from the electrical grid.

#### 2.4.3. Hydrogen exergy cost

The water electrolyzer technologies adopted in this work are the following: alkaline electrolysis (AWE), proton-exchange membrane electrolysis (PEM), solid oxide electrolysis cell (SOEC), and anion-exchange membrane electrolysis (AEM). Each one of them had their operation and infrastructure material intensity evaluated based on diverse Refs. [2,14,25,31,35]. The hydrogen exergy costs follow the approach presented on [15,32]. Table B.5 presents the infrastructure material intensity estimations for each technology, whereas Table B.6 in Appendix B presents the operation parameters adopted for them. An yearly operation working time of 8760 h was assumed in our analysis. With the electrolyzers parameters in hand, we estimated the exergy costs of producing hydrogen based on the leveled exergy cost of electricity (LExCOE) for 14 different combinations of PES with grid. The hydrogen exergy cost from AWE, PEM, SOEC, and AEM are available on Appendix B.

#### 2.4.4. Nitrogen exergy cost

The authors evaluated the exergy cost of nitrogen for the proposed GAP via adopting a cryogenic air separation unit (ASU) [39]. The adopted exergy efficiency was 0.1473 and the consumed electricity comes from the same origins as the ammonia plant (same LExCOE). Thus, Table B.13 (on Appendix B) presents the estimated exergy costs of obtaining stream 2 at the composition presented on Table A.3 for each IEA scenario combined with each electricity source case.



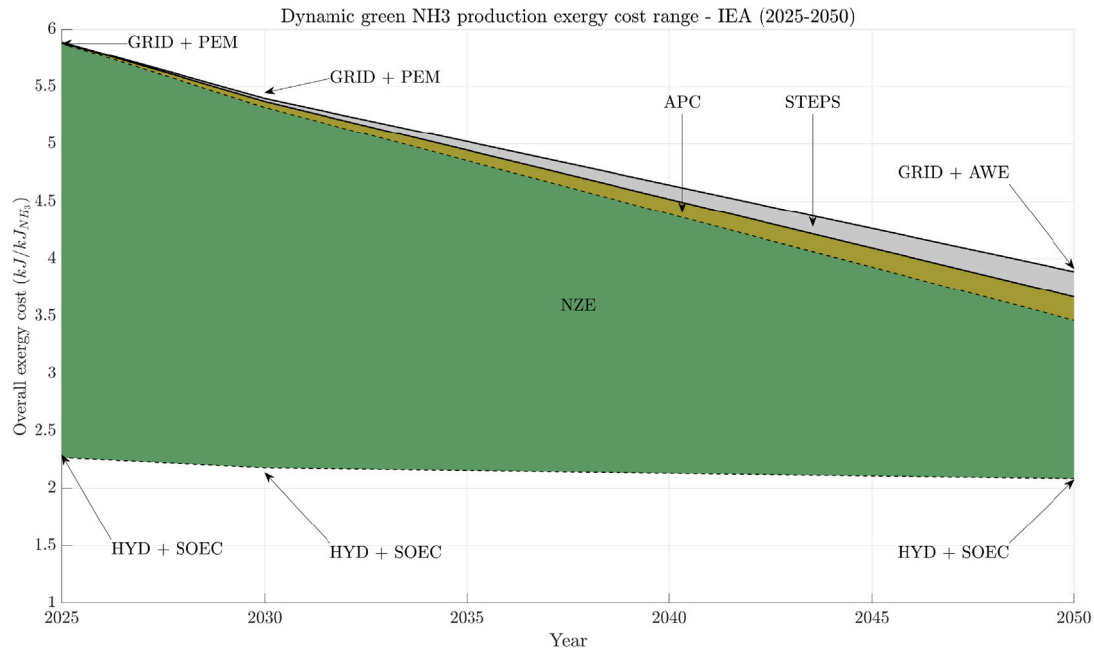


Fig. 3. Range of projected green ammonia production unit exergy costs (unit: kJ/kJ<sub>NH<sub>3</sub></sub>) under IEA projected scenarios (2025–2050). The superior and inferior lines represent the maximum and minimum values of unit exergy costs for each energy transition scenario. Green represents NZE, yellow APC and gray STEPS.

### 3. Results and discussion

#### 3.1. Thermo-economic costs

Table 1 presents the thermo-economic performance of our plant, thus allowing us to provide realistic exergy costs to our GAP inputs and evaluate the cost allocation over the plant streams. The mixing processes did not contribute to exergy destruction, as indicated by their very low unit exergy cost. In terms of heating and cooling, the heat transfer units (especially HEX 1) were responsible for the lowest exergy efficiency and thus the highest unit exergy cost (28.3% and 3.535 kJ/kJ, respectively) found on the plant simulation. As shown by Table A.3, HEX1 heat transfer occurred close to the reference temperature for both water and feed streams — fundamental factor to the poor unit exergy performance. Lastly, the innate irreversibility of a separation process caused the highest exergy destruction among all productive processes (around 638 kW), thus collaborating for the increase of the unit exergy cost of our main product, liquid ammonia (1.544 kJ/kJ<sub>NH<sub>3</sub></sub>).

#### 3.2. Dynamic green ammonia exergy cost/specific exergy consumption under the IEA energy transition scenarios

In this section, we expanded the view of our system by including the non-renewable and renewable exergy costs of both the plant's main inputs and the required infrastructure for obtaining them (from all PES systems and water electrolyzers technologies) in a circular thermo-economic analysis. The goal is to include not only the operation performance into consideration but also the physical costs of obtaining required materials to be able to yield ammonia under described conditions.

Fig. 3 presents a range of overall unit exergy costs of producing NH<sub>3</sub> under all studied IEA scenarios from 2025 up to 2050. All 14 energy technology combination cases and 4 water electrolysis technologies presented on Tables B.6–B.9 are included in this analysis. It is noteworthy how the PES affects the unit exergy cost of obtaining pure ammonia on 2025: these can be as low as 2.3 kJ/kJ<sub>NH<sub>3</sub></sub> or as high as 5.9 kJ/kJ<sub>NH<sub>3</sub></sub>, as are the cases of hydro and SOEC and electricity grid

Table 1

Thermo-economic analysis for the plant base-case.

| Unit Op. | F (kW)   | P (kW)   | I (kW)  | k (kJ/kJ) | $\eta_{2nd}$ (%) |
|----------|----------|----------|---------|-----------|------------------|
| MIX1     | 7327.45  | 7212.13  | 55.32   | 1.0076    | 99.24            |
| MIX2     | 40598.29 | 40573.15 | 25.14   | 1.0006    | 99.94            |
| MIX3     | 41803.60 | 41732.22 | 71.38   | 1.0017    | 99.83            |
| MIX4     | 336.63   | 336.63   | 0.00    | 1.0000    | 100.00           |
| MIX5     | 1687.99  | 1687.99  | 0.00    | 1.0000    | 100.00           |
| SPLIT1   | 41608.60 | 41608.60 | 0.00    | 1.0000    | 100.00           |
| SPLIT2   | 33662.80 | 33662.80 | 0.00    | 1.0000    | 100.00           |
| COMP1    | 808.58   | 660.68   | 147.90  | 1.2239    | 81.71            |
| COMP2    | 568.34   | 471.52   | 96.82   | 1.2053    | 82.96            |
| HEX1     | 96.76    | 27.37    | 69.39   | 3.5354    | 28.29            |
| HEX2     | 284.50   | 224.85   | 59.64   | 1.2652    | 79.04            |
| HEX3     | 580.38   | 400.75   | 179.63  | 1.4482    | 69.05            |
| HEX4     | 55.12    | 55.12    | 0.00    | 1.0000    | 100.00           |
| REAC1    | 21029.15 | 20999.30 | 29.85   | 1.0014    | 99.86            |
| REAC2    | 41732.22 | 41673.96 | 58.27   | 1.0014    | 99.86            |
| SEP1     | 7091.16  | 6452.62  | 638.54  | 1.0990    | 91.00            |
| ENV      | 9964.24  | 6452.62  | 3511.62 | 1.5442    | 64.76            |

and PEM, respectively. Over time, there is a significant reduction on the exergy costs of renewable energy production and thus on hydrogen. They range from 2.1 to 3.5 kJ/kJ<sub>NH<sub>3</sub></sub> under the NZE scenario presents the lowest costs due to the rapid decarbonization and reduction of non-renewable energy sources reliance on the overall production chain. APC and STEPS 2050's values are higher, with upper boundaries of 3.7 and 3.9 kJ/kJ<sub>NH<sub>3</sub></sub>, respectively. The differences between the shaded areas indicate the extra unit exergy/physical costs that we will pay (with materials, inefficiencies, carbon footprint) to produce ammonia under these scenarios (more than 11% higher). Although the highest values found for 2025 and 2030 were found for the grid and PEM combo, in 2050 this scenario changes to AWE, emphasizing the long-range evolution limitations of AWE. Also, this figure highlights how strong the combo GAP + renewables (especially hydro) + SOEC can be, although uncertainties arise on SOEC's immediate application and on hydro's availability in most places of the world.

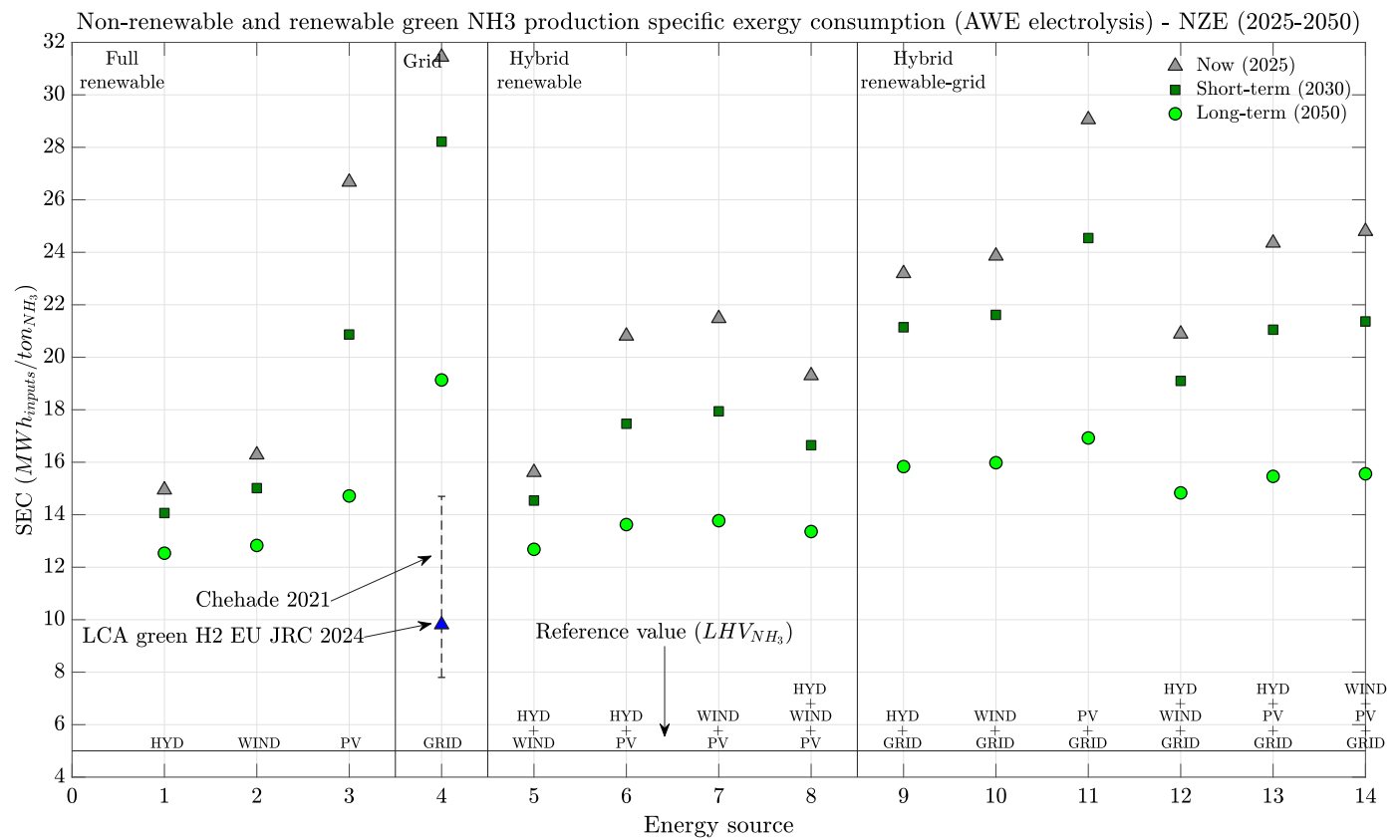


Fig. 4. Current, short-term, and long-term projected green ammonia production specific exergy consumption (SEC) for AWE electrolysis under the IEA-NZE scenario (2025–2050). X-axis represents possible fits between renewable energy source (hydro, wind, and solar PV) electricity and grid electricity used to both yield hydrogen and to feed the GAP.

Fig. 4 represents current (2025), short-term (2030), and long-term (2050) projected green ammonia production specific exergy consumption (SEC, MWh/t<sub>NH<sub>3</sub></sub>) for AWE electrolysis under the IEA-NZE scenario. Here we present the results from all 14 different electricity source cases (fully renewable, full electrical grid, hybridization between renewables, and hybridization between renewables and the electricity grid) presented on Table B.9. The idea lies in covering the most range of electricity sources possibilities for ammonia production. In order to validate the renewable and non-renewable exergy costs of producing ammonia on our current plant configuration and restrictions, we compared our SEC with (energy-based) reference values found on [1] for gray and blue ammonia plants of different scales (7.8:14.7 MWh/t<sub>NH<sub>3</sub></sub>, operation only) and with values from producing green NH<sub>3</sub> from an EU JRC's green H<sub>2</sub> environmental LCA report [40] (approximately 9.88 MWh/t<sub>NH<sub>3</sub></sub>). It is clear that there are electricity technology alternatives that fit under this range of values, especially at 2050. Although the basis is not the same, it is noticeable that how these exergy costs physically compare to current ammonia production industries.

Another important thing to note is how the exergy costs decrease for all production scenarios. For example, using hydro as the only electricity source provides the lowest exergy costs of producing liquid among all studied alternatives (from 15.0 to 12.5 MWh/t<sub>NH<sub>3</sub></sub>). Wind provides similar results, reaching out a 20% reduction. However, wind has more potential regions than hydro (currently found in China, Brazil, Canada, the US, etc.), and it is already diffused [38,41,42]. Solar PV presents the highest cost reduction over time (from 29.0 to almost 15.0 MWh/t<sub>NH<sub>3</sub></sub>, 50%) and it is the most available among the three. Besides, future projections indicate a continuous cost decrease up to 2050 [2]. Therefore, wind and solar PV are two important options to turn GAP plants economically and technically viable, especially for regions such as Spain, that possess the most abundant renewable energy potential surplus between all EU countries [41]. In summary, these trends of

renewables can be mainly justified by two factors: the infrastructure costs reduction due to the increase of renewables, and improvement on their efficiency and lifespan. It is important to clarify that we assumed a steady-state plant operation — difficult condition to happen with only renewables because of the renewables production intermittency. Without a robust hydrogen storage unit, the plant performance will be even worse. However, these results show how even small-scale plants can yield green ammonia at fully renewable operation conditions and with low exergy cost, although aspects as plant infrastructure, catalysts lifespan, and renewables capacity factor variability affect and also need to be taken into account to project more realistic scenarios.

As an alternative to deal with the variability of renewables, mixing or hybridizing electricity between two or more sources has been currently suggested to improve electricity production stability [9,43]. Then, we combined hydro, wind, and solar PV's LExCOEs [25] to show how ammonia exergy costs would appear under these scenarios. It is noticeable how PV affects the exergy cost variability over time. The main reasons for PV's high cost are its lifespan (20 years in our model) and refined silicon (approximately 1400 MJ/kg) [31]. Nevertheless, its weight on the exergy costs decrease significantly over time. Wind provides intermediate exergy costs between the three, so it presents a good compromise to increase electricity and hydrogen production stability for ammonia plants. Hydro, on the other hand, depends significantly less on critical materials, possess a higher lifespan and it is a more consolidated technology, so its variance is significantly lower than the other two. However, since it is less available, its scenarios benefits only specific regions of the planet. Finally, it is to remind that these values are conservative projections, since the overall capacity factor was not affected by the combination of each renewable. Nevertheless, how the produced electricity will be managed on such systems is as equally important on mitigating electricity curtailment as having more

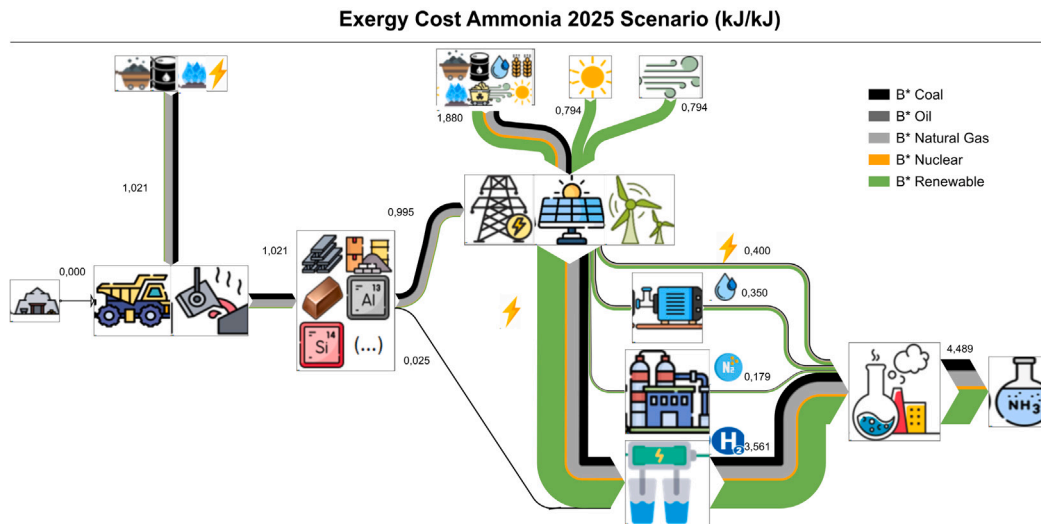


Fig. 5. Grassmann diagram of the projected green ammonia production exergy cost for the AWE + Wind + PV + electricity grid under the IEA's NZE scenario (2025) (kJ/kJ<sub>NH<sub>3</sub></sub>).

electricity available. Therefore, future investigations on how hybridizing renewable energy source systems affect the exergy costs would be useful to further approximate these costs from reality.

A further step in order to reduce the GAP load variability would be mixing the usage of electricity obtained from renewable energy systems with the electricity grid. This strategy would allow the plant to properly have electricity all the time, thus allowing it to operate at nominal conditions, but at a cost of both reducing the renewability of the overall system. Therefore, this type of ammonia would not be classified as fully green. First, we projected the exergy costs of green ammonia with only electricity grid from the NZE scenario. As decarbonization takes place, the exergy costs decrease significantly from 31.5 to 28.0 MWh/t<sub>NH<sub>3</sub></sub> (2030) and then to almost 19.0 MWh/t<sub>NH<sub>3</sub></sub> (2050). However, ammonia produced from this grid would still have significant CO<sub>2</sub> footprint depending of the region, thus propagating these to the production chain. In order to make up for this issue, hybridizing grid with local renewable energy sources seems an alternative step to mitigate the costs of electricity grid as the plant becomes more flexible in terms of hydrogen availability. In 2025, the exergy costs of all 6 studied alternatives would differ between 21.0 and 29.0 MWh/t<sub>NH<sub>3</sub></sub> (hydro, wind and grid versus PV and grid, respectively). However, this variability reduce as we approach 2050, as noticed by the values of the same alternatives (15.0 and 17.0 MWh/t<sub>NH<sub>3</sub></sub>, respectively).

### 3.3. Example of a Grassmann diagram of non-renewable and renewable exergy costs of green ammonia production

In order to show how the inputs exergy costs affect the ammonia's, the authors present a Grassmann diagram (Fig. 5) of non-renewable and renewable exergy cost contributions for scenario 14 of Table B.9 for 2025 under the IEA NZE scenario. We chose wind and PV because they have been thoroughly investigated as the most representative off-grid hybrid renewable electrical system due to its superior availability in comparison to hydroelectric sources. Also, we combined it with electricity grid to both represent a condition where the plant load would operate at nominal load and to show how electricity grid would affect the non-renewable exergy costs of ammonia.

The overall exergy cost of producing ammonia under these conditions is 4.489 kJ/kJ<sub>NH<sub>3</sub></sub>, with a non-renewable exergy cost contribution of around 40%. The sources of this non-renewable energy and carbon footprints are mostly fossil fuels consumption on mineral mining through the processes of extraction, concentration, smelting and refining [31]. Materials are required to both PES and electrolyzer infrastructures, so they naturally contribute for the exergy cost. Their

costs are represented by the value of 0.895 kJ/kJ<sub>NH<sub>3</sub></sub> originated from direct usage of fossil fuels (NG, oil and coal) and electricity from non-renewable sources on mineral mining. Therefore, they collaborate from a cradle-to-gate perspective on the PES infrastructure's exergy costs, representing 20% of the overall unit exergy cost. Both wind and solar PV depend significantly on materials for their operation (e.g., stainless steel and refined silicon are the main ones, respectively), thus the first generations of renewable infrastructures that used non-renewable energy sources on their material extraction and manufacturing still have a significant contribution on the non-renewable exergy cost of electricity [25]. On the other hand, the AWE infrastructure did not represent a significant contribution on the overall NH<sub>3</sub> exergy cost (less than 0.5%), as noticed by the value of 0.025 kJ/kJ<sub>NH<sub>3</sub></sub>. Even though their materials also have non-renewable origins, AWE does not depend on critical raw materials (except Ni), thus its material intensities B.5 do not weight on the overall H<sub>2</sub> and NH<sub>3</sub> exergy costs as much as PGMs affect PEM's, for example. The energy intensities to obtain these rare elements [31] combined with the non-renewable energy usage on their extraction increase their overall infrastructure physical cost and thus affect the whole product chain. Finally, in terms of electricity sources, the non-renewable contribution comes from part of the electricity grid that is obtained from fossil fuels and nuclear energy (1.880 kJ/kJ<sub>NH<sub>3</sub></sub>). These values are propagated on separating N<sub>2</sub>, pumping cooling water, feeding the ammonia synthesis compressors and to produce H<sub>2</sub> from electrolysis. This diagram would change over time based on how the energy transition scenario goes on in the next years (as Fig. 4 highlights), likely reducing the exergy cost of ammonia due to the increasing renewability of the electrical sector.

### 3.4. Comparison between different water electrolysis technologies

Fig. 6 presents green ammonia's exergy costs for a solar-PV plant for all electrolysis technologies under the three IEA scenarios. The projected SOEC's energy efficiency provides the lowest exergy costs (from 22.0 to around 13.5 MWh/t<sub>NH<sub>3</sub></sub>), even though its current lifespan is significantly lower than more consolidated technologies such as AWE and PEM. Thus, it is clear that SOEC's infrastructure does not weigh on the costs, since it does not significantly depend on rare metals usage. Furthermore, the heat integration potential would allow the production of steam, consequently reducing ammonia's overall cost. However, it is still under R&D [12,13]. The other three electrolyzers present similar values, ranging from 27:28 to 14.5:15.5 MWh/t<sub>NH<sub>3</sub></sub>. AEM presents somewhat better values than PEM (difference of 0.3 MWh/t<sub>NH<sub>3</sub></sub>) due to the weight of PGMs exergy costs. However, AEM

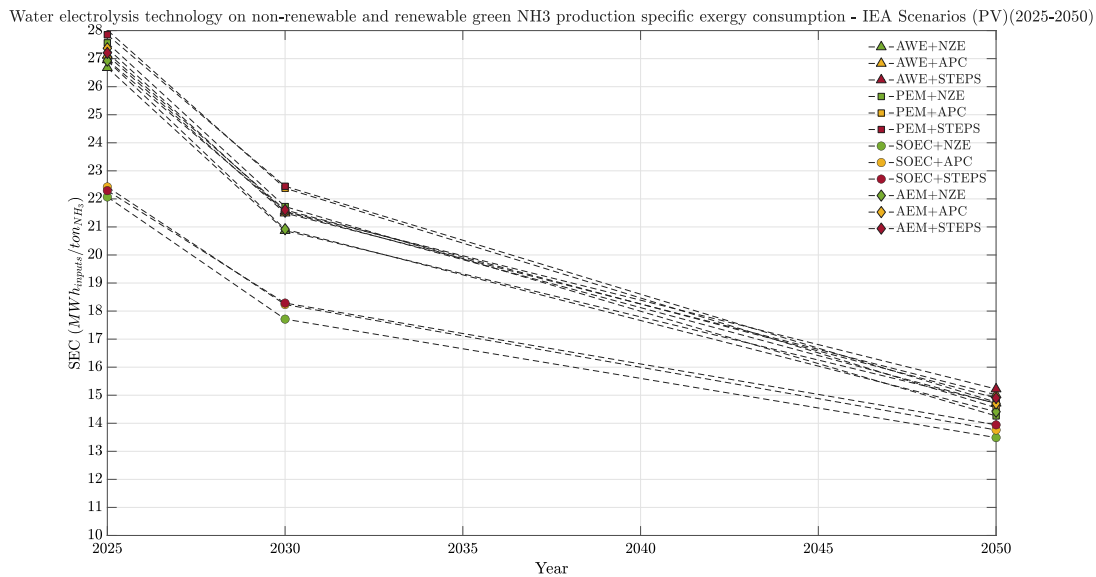


**Fig. 6.** Current, short-term, and long-term projected green ammonia production specific exergy consumption (SEC) for different water electrolysis technologies under IEA's NZE, APC, or STEPS scenarios (2025–2050). X-axis represents time (in years). The legend classifies between each water electrolysis (alkaline water electrolysis — AWE, triangle icon, proton-exchange membrane electrolysis — PEM, square icon, solid oxide electrolysis cell — SOEC, circle icon, or anion-exchange membrane electrolysis — AEM, diamond icon) and IEA energy transition scenario (NZE — green, APC — orange, STEPS — red).

is still in its infancy (low TRL) and also needs further development for commercial applications. AWE's 2025 exergy costs are lower than PEM and AEM (lower than  $27.0 \text{ MWh/t}_{\text{NH}_3}$ ), mainly because it is a consolidated technology not so dependent of critical raw materials (mainly Ni), and with similar efficiencies and higher lifespan than them. However, on the long run, PEM and AEM overcome this situation, presenting lower exergy costs. Lastly, some points need to be clarified about PEM. First, it is the technology that shows the highest exergy cost reduction. Although it appears to provide intermediate costs, it provides the best electricity load fluctuation response and therefore the most flexibility [44], and advancements on mitigating the usage of PGMs on its infrastructure for less rare materials will likely consolidate its position as a safe choice regarding hydrogen and green ammonia.

### 3.5. Discussion of restrictions and future possibilities

In the context of our studied plant, it is a known fact that small-scale GAPs can neither compete financially (CAPEX and OPEX) nor technically (i.e., efficiency or size production) with current gray ammonia plants due to the economy of scale factor [1,6]. Additionally, energy curtailment is an additional issue for all sectors that depend on renewables (and naturally to the green ammonia production) [45]. However, in order to evaluate how renewable this type of chemical plants can be and how they affect the planetary boundary limits [46], natural resources availability [47] and their physical/exergy costs should be accounted on this evaluation. It is thus fundamental to operate small-scale GAPs based on the fundamentals of industrial symbiosis to find its economical, technical and environmental optimal points. Therefore, next we discuss some intricate aspects of these plants that require proper attention to reach the aforementioned goals of our text.

#### 3.5.1. Renewable energy hybridization

As previously mentioned, novel configurations of green hydrogen plants have been projected with hybrid renewable energy sources to obtain a more stable electricity management system in order to reduce electricity curtailment while being small-cost and simple in operation [48]. More specifically for GAPs, this can assist on keeping the plant load stable over time. One interesting alternative studied here is the combination of solar PV with wind energy, where PV plants can assist on the (more) erratic and volatile behavior of wind plants, whereas wind's higher efficiency can make up the lower efficiency of PV's [9,43].

#### 3.5.2. Hydrogen alternatives

In Europe, if a 100%  $\text{CO}_2$  emissions reduction is required for such plants, current levelized hydrogen costs for hydrogen/ammonia plants will dramatically increase (around  $6.3 \text{ €/kg}_{\text{H}_2}$ ) and consequently these will occupy more land surface area for renewables [49]. Thus, other pathways to sustainable low-carbon hydrogen sources other than water electrolysis have been discussed on literature, such as biomass [4] and natural hydrogen [50] from geological reserves. These can collaborate to decarbonize the current ammonia production sector. Some questions need to be addressed, though. Since biomass comes originally from agriculture, the inclusion of land and soils as non-renewable natural resources would complicate the discussion when evaluating the ecological footprints of ammonia produced by this pathway. In the case of natural hydrogen, its reserves are particularly scarce around the world [51,52], but techno-economic studies about hydrogen extraction have already been proposed [53]. These resources also need to be investigated for its non-renewable and renewable exergy costs on renewable ammonia plants in order to confirm its environmental, physical, technical, and economical viabilities.

#### 3.5.3. Technical aspects and byproducts

Fundamental technical aspects internal to GAPs are important to their OPEX and ecological footprint [4,19,21]. These involve material/energy integration between GAP, green hydrogen, and ASU plants, and the inclusion of renewable energy production fluctuation over the year. Industrial symbiosis via byproducts for self-usage or other industries with hydrogen, oxygen, and argon recoveries [54] would enhance the plant overall efficiency and reduce their exergy costs. SOEC systems could also be thermally integrated with subsequent chemical plant production systems [12,13]. For example, stream 25 (water-steam mixture, 5%) is another residue from our plant that has an interesting potential to be further recovered and could be converted into either saturated or super-heated vapor. Additionally, the purge stream 20, whose composition is 59.4% hydrogen, 19.7% nitrogen, 14.2% ammonia, and 6.6% argon, has components with technical value and importance [55]. Therefore, why not take advantage of such an argon-rich stream to separate and obtain it as a byproduct? In our work, the purge stream exergy cost ranged around 1.90 to 5.36  $\text{kJ/kJ}_{\text{purge}}$ , which is already advantageous in comparison to some ASUs 19.5  $\text{KWh/kg}$  [39]. In addition, alternatives for this issue such as new



**Table A.2**  
Inputs/set points of the designed ammonia synthesis plant.

| Parameter         | Description  | Values                       |
|-------------------|--|------------------------------|
| $\dot{n}(1)$      | Hydrogen stream molar flow rate [kmol/h]                   | 106.92                       |
| $T(1)$            | Hydrogen stream temperature [K]                            | 300.0                        |
| $p(1)$            | Hydrogen stream pressure [bar]                             | 30.0                         |
| $[y(1)]$          | Hydrogen stream composition [kmol/kmol]                    | [100mol% $H_2$ ]             |
| $\dot{n}(2)$      | Hydrogen/nitrogen ratio [ $H_2/N_2$ ]                      | 3:1                          |
| $T(2)$            | Nitrogen stream temperature [K]                            | 300.0                        |
| $[y(2)]$          | Nitrogen stream composition [kmol/kmol]                    | [99.0mol% $N_2$ , 1.0mol%Ar] |
| $p(5)$            | First-stage compressor pressure [bar]                      | 100.0                        |
| $T(6)$            | Outlet hot-side intercooler temperature [K]                | 350.0                        |
| $p(7)$            | Second-stage compressor pressure [bar]                     | 200.0                        |
| $\eta_{COMP}$     | Compressors isentropic efficiency [–]                      | 0.8                          |
| $T(10)$           | Inlet first bed reactor temperature [K]                    | 630.0                        |
| $p(10)$           | Inlet first bed reactor pressure [bar]                     | 200.0                        |
| $T(12)$           | Inlet second bed reactor temperature [K]                   | 602.5                        |
| $p(12)$           | Inlet second bed reactor pressure [bar]                    | 190.0                        |
| $\Delta p_{REAC}$ | Total reactor pressure drop [bar]                          | 10.0                         |
| $T(15)$           | Outlet water cooler temperature [K]                        | 350.0                        |
| $T(16)$           | Outlet air cooler temperature [K]                          | 300.0                        |
| $p(30)$           | Separator pressure [bar]                                   | 30.0                         |
| $\dot{Q}_{REAC}$  | Reactor heat rate (adiabatic) [kW]                         | 0                            |
| $r_{quench}$      | Quench flow ratio [–]                                      | 0.5                          |
| $r_{purge}$       | Purge flow ratio [–]                                       | 0.01                         |
| $L_{REAC1}$       | First-bed reactor length [m]                               | 3.150                        |
| $V_{REAC1}$       | First-bed reactor volume [m <sup>3</sup> ]                 | 1.500                        |
| $L_{REAC2}$       | Second-bed reactor length [m]                              | 6.300                        |
| $V_{REAC2}$       | Second-bed reactor volume [m <sup>3</sup> ]                | 2.900                        |
| $k_f$             | Forward reaction coefficient [kmol/(kg <sub>cat</sub> h)]  | 8.5E4                        |
| $n_f$             | Forward reaction exponent [–]                              | 0                            |
| $E_{act,f}$       | Forward reaction activation energy [kJ/kmol]               | 8.709E4                      |
| $k_b$             | Backward reaction coefficient [kmol/(kg <sub>cat</sub> h)] | 1.22E17                      |
| $n_b$             | Backward reaction exponent [–]                             | 0                            |
| $E_{act,b}$       | Backward reaction activation energy [kJ/kmol]              | 1.98464E5                    |

cryogenic ASU configurations for obtaining noble gases [56] or pressure swing adsorption (PSA) systems [57,58] are already available. Another possible byproduct of this plant is the oxygen gas [59]. An industrial symbiosis between the metallurgic and ammonia sectors would greatly benefit them.

### 3.5.4. Limitations and future works

Finally, it is important to clarify some limitations of the current study. CO<sub>2</sub> emissions were not included here, and naturally its evaluation and the exergy costs required to turn these plants carbon-neutral can be beneficial as well. Cooling water exergy costs have been considered [37], however without accounting for the LExCOE concept of infrastructures. The exergy costs linked to the demand of deionized water from PEM systems have not been included either. Thus, industrial processes should account for non-renewable exergy footprint when using water from different origins, especially with the energy transition scenario is projecting enormous amounts of water to be converted in hydrogen [60].

Future studies will focus on reducing the non-renewable exergy costs of processes. An important addition to this analysis is how to add soils and land as a non-renewable natural resources and how to use exergy to evaluate this concept [61]. Others briefly mentioned here are: investigations involving LExCOE and ammonia's costs under distinct natural resources availability due to location (groundwater or seawater availability, natural H<sub>2</sub>, soil exergy, renewables and weather variation), dynamic simulations for different plant load operations [62], electricity curtailment management and control, and inclusion of the non-renewable exergy costs of the electrolyzers manufacturing process [14], different catalysts, the plants storage or overall infrastructure [40] on the overall exergy cost, and novel ammonia different separation methods (adsorption or membranes). How to compare soil/land usage for solar PVs or wind turbines to obtain renewable electricity, or to plant and harvest food for us to live, or to keep the forests, biodiversity, water basins [60] and capture CO<sub>2</sub> [63]? Some questions still need to be answered.

## 4. Conclusions

We evaluated the overall exergy costs of small-scale GAP whose input exergy costs were based on the LExCOE approach for IEA's future energy transition scenarios between 2025 and 2050. Projections of four water electrolysis technology efficiencies, ASU and distinct PES electricity exergy costs allowed us to obtain the exergy costs of green hydrogen, green nitrogen, and electricity and consequently to evaluate the exergy cost of ammonia under diverse conditions.

Results covered 504 different scenarios of liquid ammonia production, where the most interesting and attractive involved the combination hydro and SOEC with an overall exergy cost of 2.1 kJ/kJ<sub>NH<sub>3</sub></sub> or 12.5 MWh/t<sub>NH<sub>3</sub></sub> in 2050 for the NZE pathway. Solar PV scenarios presented the highest exergy costs among the individual renewable energy sources due to its current high exergy cost associated with infrastructure, whereas wind presents as a very flexible alternative in terms of exergy costs to be adopted in most places of the world. AWE exergy costs are interesting in terms of immediate implementation due to its commercial availability and to not be dependent on critical raw materials usage, such as PEMs are. However, it presents worse exergy costs in the long run when compared to all the rest. SOEC presents the best performance at all moments, but its low TRL increases the uncertainty to its short-term application on industrial scale.

The simulated GAP yielded high-purity ammonia with an exergy efficiency of 64% (or 1.54 kJ/kJ<sub>NH<sub>3</sub></sub>) and with potential to be more efficient and economically attractive with proper attention to its byproducts (e.g., purge stream, with argon production, hydrogen, and ammonia recovery). Industrial symbiosis possibilities were discussed as well, with highlight to the need of hybridization of renewable energy production. Our findings present possibilities where these type of plants can operate based on local renewables availability for regional ammonia production for fertilizers or energy storage. A full plant representation under transient conditions with hybrid renewable energy systems, energy storage via batteries and hydrogen, production and storage, electricity curtailment is on the scope of this research. Also, overall CO<sub>2</sub>

**Table A.3**

Stream table summarizing the main thermodynamic properties (exergy flow, enthalpy, entropy, and overall mole fraction) of all streams involved in the plant.

| Stream        | $\dot{B}$<br>[kW] | h<br>[ $\frac{\text{kJ}}{\text{kg}}$ ] | s<br>[ $\frac{\text{kJ}}{\text{kg K}}$ ] | $x_{\text{H}_2}$<br>[–] | $x_{\text{N}_2}$<br>[–] | $x_{\text{NH}_3}$<br>[–] | $x_{\text{Ar}}$<br>[–] |
|---------------|-------------------|--|--|-------------------------|-------------------------|--------------------------|------------------------|
| 1             | 7236.7            | 39.5                                   | –13.92                                   | 1                       | 0                       | 0                        | 0                      |
| 2             | 90.7              | –4.1                                   | –1.00                                    | 0                       | 9.90E–01                | 0                        | 1.00E–02               |
| 3             | 7272.1            | 3.58                                   | –2.72                                    | 7.48E–01                | 2.49E–01                | 0                        | 2.52E–03               |
| 4             | 40 573.2          | –522.98                                | –3.00                                    | 6.28E–01                | 2.09E–01                | 1.11E–01                 | 5.21E–02               |
| 5             | 41 233.8          | –115.70                                | –2.75                                    | 6.28E–01                | 2.09E–01                | 1.11E–01                 | 5.21E–02               |
| 6             | 41 137.1          | –328.50                                | –3.30                                    | 6.28E–01                | 2.09E–01                | 1.11E–01                 | 5.21E–02               |
| 7             | 41 608.6          | –42.23                                 | –3.14                                    | 6.28E–01                | 2.09E–01                | 1.11E–01                 | 5.21E–02               |
| 8             | 20 804.3          | –42.23                                 | –3.14                                    | 6.28E–01                | 2.09E–01                | 1.11E–01                 | 5.21E–02               |
| 9             | 20 804.3          | –42.23                                 | –3.14                                    | 6.28E–01                | 2.09E–01                | 1.11E–01                 | 5.21E–02               |
| 10            | 21 029.2          | 469.37                                 | –2.18                                    | 6.28E–01                | 2.09E–01                | 1.11E–01                 | 5.21E–02               |
| 11            | 20 999.3          | 469.39                                 | –2.08                                    | 5.59E–01                | 1.86E–01                | 1.99E–01                 | 5.62E–02               |
| 12            | 41 732.2          | 213.57                                 | –2.39                                    | 5.95E–01                | 1.98E–01                | 1.53E–01                 | 5.40E–02               |
| 13            | 41 674.0          | 213.57                                 | –2.39                                    | 5.24E–01                | 1.74E–01                | 2.44E–01                 | 5.83E–02               |
| 14            | 41 389.5          | –42.24                                 | –2.76                                    | 5.24E–01                | 1.74E–01                | 2.44E–01                 | 5.83E–02               |
| 15            | 40 809.1          | –822.12                                | –4.40                                    | 5.24E–01                | 1.74E–01                | 2.44E–01                 | 5.83E–02               |
| 16            | 40 754.0          | –1196.28                               | –5.56                                    | 5.24E–01                | 1.74E–01                | 2.44E–01                 | 5.83E–02               |
| 17            | 6452.6            | –4083.3                                | –11.58                                   | 6.10E–04                | 2.63E–04                | 9.99E–01                 | 1.67E–04               |
| 18            | 33 662.8          | –632.26                                | –3.10                                    | 5.94E–01                | 1.97E–01                | 1.42E–01                 | 6.61E–02               |
| 19            | 336.6             | –632.26                                | –3.10                                    | 5.94E–01                | 1.97E–01                | 1.42E–01                 | 6.61E–02               |
| 20            | 336.6             | –632.26                                | –3.10                                    | 5.94E–01                | 1.97E–01                | 1.42E–01                 | 6.61E–02               |
| 21            | 33 326.2          | –632.26                                | –3.10                                    | 5.94E–01                | 1.97E–01                | 1.42E–01                 | 6.61E–02               |
| Water streams |                   |  |  |                         |                         |                          |                        |
| 22            | 1259.9            | –15 856.9                              | –9.03                                    | –                       | –                       | –                        | –                      |
| 23            | 1287.2            | –15 696.6                              | –8.53                                    | –                       | –                       | –                        | –                      |
| 24            | 1688.0            | –15 109.1                              | –7.07                                    | –                       | –                       | –                        | –                      |
| 25            | 1688.0            | –15 109.1                              | –7.07                                    | –                       | –                       | –                        | –                      |

footprint, soil exergy inclusion, purge optimization with alternative gas separation systems (novel cryogenic, PSA and membranes) are also in sight to pursue our goal of evaluating the renewability of these plants.

#### CRedit authorship contribution statement

**Alessandro Lima:** Writing – original draft, Visualization, Validation, Software, Resources, Methodology, Data curation, Conceptualization. **Jorge Torrubia:** Writing – original draft, Visualization, Software, Methodology, Data curation, Conceptualization. **César Torres:** Software, Methodology. **Alicia Valero:** Supervision. **Antonio Valero:** Supervision, Methodology, Conceptualization.

#### Declaration of competing interest

The authors declare that they have no known competing financial interests or personal relationships that could have appeared to influence the work reported in this paper.

#### Acknowledgments

This research has been funded by both the NextGeneration EU under the Renewable Energy and Hydrogen Complementary Plan (GA no. 2022/4/0042, Order PRI/1762/2022, of October 27th, by MICIU/AEI/10.13039/501100011033), and FEDER (EU) under grant agreements for RESTORE (PID2023-148401OB-I00) and FUTURE GREEN AMMONIA (CPP2023-010756).

#### Appendix A. Ammonia plant data

See [Tables A.2–A.4](#).

#### Appendix B. IEA scenarios summary data, electrolyzer parameters, dynamic exergy costs of electricity (LEXCOE), hydrogen and nitrogen for all evaluated water electrolysis technologies

See [Tables B.5–B.13](#).

**Table A.4**

Fuel-product equations of all equipment/unit operations in study (where  $I = F - P$ ).

| Equipment | Fuel ( $F$ )                  | Product ( $P$ )               | Type        |
|-----------|-------------------------------|-------------------------------|-------------|
| MIX1      | $\dot{B}_1 + \dot{B}_2$       | $\dot{B}_3$                   | Productive  |
| MIX2      | $\dot{B}_3 + \dot{B}_{21}$    | $\dot{B}_4$                   | Productive  |
| MIX3      | $\dot{B}_8 + \dot{B}_{11}$    | $\dot{B}_{12}$                | Productive  |
| MIX4      | $\dot{B}_{19}$                | $\dot{B}_{20}$                | Dissipative |
| MIX5      | $\dot{B}_{24}$                | $\dot{B}_{25}$                | Dissipative |
| SPLIT1    | $\dot{B}_7$                   | $\dot{B}_8 + \dot{B}_9$       | Productive  |
| SPLIT2    | $\dot{B}_{18}$                | $\dot{B}_{19} + \dot{B}_{21}$ | Productive  |
| COMP1     | $\dot{B}_{26}$                | $\dot{B}_5 - \dot{B}_4$       | Productive  |
| COMP2     | $\dot{B}_{27}$                | $\dot{B}_7 - \dot{B}_6$       | Productive  |
| HEX1      | $\dot{B}_5 - \dot{B}_6$       | $\dot{B}_{23} - \dot{B}_{22}$ | Productive  |
| HEX2      | $\dot{B}_{13} - \dot{B}_{14}$ | $\dot{B}_{10} - \dot{B}_9$    | Productive  |
| HEX3      | $\dot{B}_{14} - \dot{B}_{15}$ | $\dot{B}_{24} - \dot{B}_{23}$ | Productive  |
| HEX4      | $\dot{B}_{15} - \dot{B}_{16}$ | $\dot{B}_{28}$                | Dissipative |
| REAC1     | $\dot{B}_{10}$                | $\dot{B}_{11}$                | Productive  |
| REAC2     | $\dot{B}_{12}$                | $\dot{B}_{13}$                | Productive  |
| SEP       | $\dot{B}_{16} - \dot{B}_{18}$ | $\dot{B}_{17}$                | Productive  |

**Table B.5**

Material intensities of the infrastructure of each water electrolysis technology. Unit in kg/MW. References: [\[2,14,35\]](#).

| Material | AWE    | PEM    | SOEC | AEM  |
|----------|--------|--------|------|------|
| Al       | 300    | 300    | 0    | 0    |
| Cu       | 1330   | 100    | 100  | 0    |
| Fe       | 0      | 0      | 143  | 0    |
| Ir       | 0      | 1.97   | 0    | 0    |
| La       | 0      | 0      | 126  | 0    |
| Ni       | 12 660 | 0      | 413  | 1660 |
| Pd       | 0      | 0.700  | 0    | 0    |
| Pt       | 0      | 0.984  | 0    | 1.6  |
| Sn       | 0      | 0      | 12.6 | 0    |
| Y        | 0      | 0.7    | 155  | 0    |
| Zr       | 100    | 0      | 302  | 0    |
| S. Steel | 33 300 | 19 500 | 9930 | 1200 |
| Glass    | 0      | 0      | 700  | 0    |
| Graphite | 287    | 4400   | 0    | 0    |

**Table B.6**

Water electrolyzer technologies operation parameters adopted in this study. References: [2,12,14,15,35].

| Parameter   | AWE     | PEM     | SOEC    | AEM     |
|---|---------|---------|---------|---------|
| $\eta_{\text{electrolyzer}}$ (2021) [35]                  | 0.5470  | 0.5341  | 0.7197  | 0.5339  |
| $\eta_{\text{electrolyzer}}$ (2050) [35]                  | 0.7407  | 0.7768  | 0.8333  | 0.7580  |
| $t_{\text{electrolyzer, lifespan}}$ (h) (2021) [35]       | 60 000  | 65 000  | 15 000  | 7500    |
| $t_{\text{electrolyzer, lifespan}}$ (h) (2050) [35]       | 100 000 | 110 000 | 80 000  | 100 000 |
| $T_{\text{Electrolyzer}}$ ( $^{\circ}\text{C}$ ) [12]     | 70–90   | 50–80   | 700–850 | 40–60   |
| $p_{\text{Electrolyzer}}$ (bar) [12]                      | <30     | <50     | 1       | <35     |
| $J_{\text{Electrolyzer}}$ ( $\text{A}/\text{cm}^2$ ) [12] | 0.2–0.8 | 1–3     | 0.3–1.0 | 0.2–2   |
| $U_{\text{Electrolyzer}}$ (V) [12]                        | 1.4–3   | 1.4–2.3 | 1.0–1.5 | 1.4–2.0 |
| $\dot{W}_{\text{elec, demonstr.}}$ (MW) [14]              | 150     | 10      | 1       | 4       |
| CAPEX ( $\text{€}/\text{kW}$ ) [14]                       | 600     | 900     | 2130    | 1000    |

**Table B.7**IEA NZE, APC and STEPS world electricity and CO<sub>2</sub> emissions scenarios summary.

Source: Data from [33].

| Parameter                  | IEA Outlook 2024 [33] | STEPS    | APC      | NZE      |
|----------------------------|-----------------------|----------|----------|----------|
|                            | 2023                  | 2050     |          |          |
| Total CO <sub>2</sub> (Mt) | 37 723.1              | 0.0      | 11 710.6 | 28 635.6 |
| Renewables (TWh)           | 9028.7                | 70 962.7 | 58 611.3 | 42 770.2 |
| Share renewables TWh (%)   | 30.2                  | 88.5     | 83.1     | 73.3     |
| Renewables (GW)            | 4246.2                | 33 178.8 | 29 355.3 | 23 218.0 |
| Share renewables GW (%)    | 45.0                  | 80.3     | 78.1     | 73.9     |

**Table B.8**

Projected levelized exergy cost of electricity (LExCOE) for combinations of primary energy sources (PES) with grid under the IEA NZE, APC and STEPS energy transition scenarios. Based on the methodology presented on [32] (Unit: kJ/kJ).

| LExCOE (kJ/kJ)     | NZE    |        |        | APC    |        |        | STEPS  |        |        |
|--------------------|--------|--------|--------|--------|--------|--------|--------|--------|--------|
| PES + Grid         | 2025   | 2030   | 2050   | 2025   | 2030   | 2050   | 2025   | 2030   | 2050   |
| 1 - HYD            | 1.0612 | 1.0573 | 1.0454 | 1.0613 | 1.0576 | 1.0460 | 1.0614 | 1.0580 | 1.0470 |
| 2 - WIND           | 1.1713 | 1.1408 | 1.0747 | 1.1642 | 1.1376 | 1.0751 | 1.1575 | 1.1323 | 1.0771 |
| 3 - PV             | 2.0279 | 1.6559 | 1.2620 | 2.0639 | 1.7103 | 1.2916 | 2.0505 | 1.7157 | 1.3115 |
| 4 - GRID           | 2.4204 | 2.3025 | 1.7009 | 2.4233 | 2.3261 | 1.8132 | 2.4242 | 2.3380 | 1.9325 |
| 5 - HYD+WIND       | 1.1163 | 1.0990 | 1.0601 | 1.1127 | 1.0976 | 1.0606 | 1.1095 | 1.0952 | 1.0621 |
| 6 - HYD+PV         | 1.5446 | 1.3566 | 1.1537 | 1.5626 | 1.3840 | 1.1688 | 1.5559 | 1.3869 | 1.1792 |
| 7 - WIND+PV        | 1.5996 | 1.3983 | 1.1684 | 1.6140 | 1.4240 | 1.1834 | 1.6040 | 1.4240 | 1.1943 |
| 8 - HYD+WIND+PV    | 1.4201 | 1.2847 | 1.1274 | 1.4298 | 1.3019 | 1.1376 | 1.4231 | 1.3020 | 1.1452 |
| 9 - HYD+GRID       | 1.7408 | 1.6799 | 1.3731 | 1.7423 | 1.6918 | 1.4296 | 1.7428 | 1.6980 | 1.4898 |
| 10 - WIND+GRID     | 1.7959 | 1.7217 | 1.3878 | 1.7937 | 1.7319 | 1.4441 | 1.7909 | 1.7352 | 1.5048 |
| 11 - PV+GRID       | 2.2242 | 1.9792 | 1.4815 | 2.2436 | 2.0182 | 1.5524 | 2.2373 | 2.0269 | 1.6220 |
| 12 - HYD+WIND+GRID | 1.5510 | 1.5002 | 1.2737 | 1.5496 | 1.5071 | 1.3114 | 1.5477 | 1.5094 | 1.3522 |
| 13 - HYD+PV+GRID   | 1.8365 | 1.6719 | 1.3361 | 1.8495 | 1.6980 | 1.3836 | 1.8453 | 1.7039 | 1.4303 |
| 14 - WIND+PV+GRID  | 1.8732 | 1.6997 | 1.3459 | 1.8838 | 1.7247 | 1.3933 | 1.8774 | 1.7287 | 1.4404 |

**Table B.9**

Projected exergy costs of hydrogen via alkaline water electrolysis (AWE) based on the levelized exergy cost of electricity (LExCOE) for combinations of primary energy sources (PES) with grid under the IEA NZE, APC and STEPS energy transition scenarios [2,32,33] (Unit: kJ/kJ).

| H <sub>2</sub> exergy cost (kJ/kJ)  |               | NZE   |       |       | APC   |       |       | STEPS |       |       |
|-------------------------------------|---------------|-------|-------|-------|-------|-------|-------|-------|-------|-------|
| Water electrolyzer technology + PES |               | 2025  | 2030  | 2050  | 2025  | 2030  | 2050  | 2025  | 2030  | 2050  |
| AWE                                 | HYD           | 1.809 | 1.667 | 1.423 | 1.809 | 1.668 | 1.424 | 1.809 | 1.669 | 1.427 |
|                                     | WIND          | 1.994 | 1.797 | 1.463 | 1.982 | 1.793 | 1.464 | 1.971 | 1.785 | 1.467 |
|                                     | PV            | 3.435 | 2.600 | 1.716 | 3.496 | 2.686 | 1.756 | 3.474 | 2.695 | 1.784 |
|                                     | GRID          | 4.096 | 3.608 | 2.308 | 4.101 | 3.646 | 2.460 | 4.103 | 3.665 | 2.622 |
|                                     | HYD+WIND      | 1.901 | 1.732 | 1.443 | 1.896 | 1.731 | 1.444 | 1.890 | 1.727 | 1.447 |
|                                     | HYD+PV        | 2.622 | 2.134 | 1.569 | 2.653 | 2.177 | 1.590 | 2.642 | 2.182 | 1.605 |
|                                     | WIND+PV       | 2.715 | 2.199 | 1.589 | 2.739 | 2.240 | 1.610 | 2.722 | 2.240 | 1.625 |
|                                     | HYD+WIND+PV   | 2.413 | 2.021 | 1.534 | 2.429 | 2.049 | 1.548 | 2.418 | 2.050 | 1.559 |
|                                     | HYD+GRID      | 2.952 | 2.638 | 1.866 | 2.955 | 2.657 | 1.942 | 2.956 | 2.667 | 2.024 |
|                                     | WIND+GRID     | 3.045 | 2.703 | 1.885 | 3.042 | 2.720 | 1.962 | 3.037 | 2.725 | 2.045 |
|                                     | PV+GRID       | 3.766 | 3.104 | 2.012 | 3.799 | 3.166 | 2.108 | 3.788 | 3.180 | 2.203 |
|                                     | HYD+WIND+GRID | 2.633 | 2.358 | 1.731 | 2.631 | 2.369 | 1.783 | 2.628 | 2.373 | 1.839 |
|                                     | HYD+PV+GRID   | 3.113 | 2.625 | 1.816 | 3.135 | 2.667 | 1.880 | 3.129 | 2.677 | 1.944 |
|                                     | WIND+PV+GRID  | 3.175 | 2.669 | 1.829 | 3.193 | 2.708 | 1.893 | 3.183 | 2.715 | 1.958 |

**Table B.10**

Projected exergy costs of hydrogen via proton-exchange membrane (PEM) electrolysis based on the levelized exergy cost of electricity (LExCOE) for combinations of primary energy sources (PES) with grid under the IEA NZE, APC and STEPS energy transition scenarios [2,32,33] (Unit: kJ/kJ).

| H <sub>2</sub> exergy cost (kJ/kJ)  |               | NZE   |       |       | APC   |       |       | STEPS |       |       |
|-------------------------------------|---------------|-------|-------|-------|-------|-------|-------|-------|-------|-------|
| Water electrolyzer technology + PES |               | 2025  | 2030  | 2050  | 2025  | 2030  | 2050  | 2025  | 2030  | 2050  |
| PEM                                 | HYD           | 1.890 | 1.759 | 1.364 | 1.891 | 1.762 | 1.365 | 1.892 | 1.763 | 1.368 |
|                                     | WIND          | 2.083 | 1.896 | 1.401 | 2.071 | 1.893 | 1.402 | 2.059 | 1.885 | 1.406 |
|                                     | PV            | 3.578 | 2.739 | 1.642 | 3.642 | 2.829 | 1.681 | 3.619 | 2.839 | 1.708 |
|                                     | GRID          | 4.264 | 3.796 | 2.207 | 4.269 | 3.837 | 2.353 | 4.271 | 3.857 | 2.508 |
|                                     | HYD+WIND      | 1.986 | 1.828 | 1.382 | 1.981 | 1.827 | 1.384 | 1.975 | 1.824 | 1.387 |
|                                     | HYD+PV        | 2.734 | 2.249 | 1.503 | 2.766 | 2.295 | 1.523 | 2.755 | 2.301 | 1.538 |
|                                     | WIND+PV       | 2.830 | 2.317 | 1.522 | 2.856 | 2.361 | 1.542 | 2.839 | 2.362 | 1.557 |
|                                     | HYD+WIND+PV   | 2.517 | 2.131 | 1.469 | 2.535 | 2.161 | 1.483 | 2.523 | 2.162 | 1.494 |
|                                     | HYD+GRID      | 3.077 | 2.778 | 1.785 | 3.080 | 2.799 | 1.859 | 3.081 | 2.810 | 1.938 |
|                                     | WIND+GRID     | 3.173 | 2.846 | 1.804 | 3.170 | 2.865 | 1.877 | 3.165 | 2.871 | 1.957 |
|                                     | PV+GRID       | 3.921 | 3.268 | 1.925 | 3.955 | 3.333 | 2.017 | 3.945 | 3.348 | 2.108 |
|                                     | HYD+WIND+GRID | 2.746 | 2.484 | 1.657 | 2.744 | 2.497 | 1.707 | 2.741 | 2.502 | 1.761 |
|                                     | HYD+PV+GRID   | 3.244 | 2.765 | 1.738 | 3.267 | 2.809 | 1.800 | 3.260 | 2.820 | 1.861 |
|                                     | WIND+PV+GRID  | 3.308 | 2.810 | 1.750 | 3.327 | 2.853 | 1.812 | 3.316 | 2.860 | 1.874 |

**Table B.11**

Projected exergy costs of hydrogen via solid oxide electrolysis cell (SOEC) based on the levelized exergy cost of electricity (LExCOE) for combinations of primary energy sources (PES) with grid under the IEA NZE, APC and STEPS energy transition scenarios [2,32,33] (Unit: kJ/kJ).

| H <sub>2</sub> exergy cost (kJ/kJ)  |               | NZE   |       |       | APC   |       |       | STEPS |       |       |
|-------------------------------------|---------------|-------|-------|-------|-------|-------|-------|-------|-------|-------|
| Water electrolyzer technology + PES |               | 2025  | 2030  | 2050  | 2025  | 2030  | 2050  | 2025  | 2030  | 2050  |
| SOEC                                | HYD           | 1.415 | 1.338 | 1.258 | 1.416 | 1.339 | 1.259 | 1.416 | 1.340 | 1.260 |
|                                     | WIND          | 1.561 | 1.443 | 1.293 | 1.552 | 1.440 | 1.294 | 1.543 | 1.433 | 1.296 |
|                                     | PV            | 2.692 | 2.091 | 1.518 | 2.739 | 2.160 | 1.553 | 2.722 | 2.167 | 1.578 |
|                                     | GRID          | 3.210 | 2.904 | 2.044 | 3.214 | 2.934 | 2.179 | 3.215 | 2.949 | 2.323 |
|                                     | HYD+WIND      | 1.488 | 1.391 | 1.275 | 1.484 | 1.390 | 1.276 | 1.479 | 1.387 | 1.278 |
|                                     | HYD+PV        | 2.054 | 1.715 | 1.388 | 2.078 | 1.750 | 1.406 | 2.069 | 1.754 | 1.419 |
|                                     | WIND+PV       | 2.126 | 1.767 | 1.405 | 2.146 | 1.800 | 1.424 | 2.132 | 1.800 | 1.437 |
|                                     | HYD+WIND+PV   | 1.889 | 1.624 | 1.356 | 1.902 | 1.646 | 1.369 | 1.894 | 1.647 | 1.378 |
|                                     | HYD+GRID      | 2.313 | 2.121 | 1.651 | 2.315 | 2.137 | 1.719 | 2.316 | 2.145 | 1.792 |
|                                     | WIND+GRID     | 2.385 | 2.174 | 1.669 | 2.383 | 2.187 | 1.736 | 2.379 | 2.191 | 1.810 |
|                                     | PV+GRID       | 2.951 | 2.497 | 1.781 | 2.977 | 2.547 | 2.866 | 2.968 | 2.558 | 1.950 |
|                                     | HYD+WIND+GRID | 2.062 | 1.895 | 1.532 | 2.060 | 1.904 | 1.577 | 2.058 | 1.908 | 1.626 |
|                                     | HYD+PV+GRID   | 3.439 | 2.111 | 1.607 | 2.456 | 2.144 | 1.664 | 2.451 | 2.152 | 1.720 |
|                                     | WIND+PV+GRID  | 2.487 | 2.146 | 1.618 | 2.502 | 2.178 | 1.675 | 2.493 | 2.183 | 1.732 |

**Table B.12**

Projected exergy costs of hydrogen via anion-exchange membrane (AEM) electrolysis based on the levelized exergy cost of electricity (LExCOE) for combinations of primary energy sources (PES) with grid under the IEA NZE, APC and STEPS energy transition scenarios [2,32,33] (Unit: kJ/kJ).

| H <sub>2</sub> exergy cost (kJ/kJ)  |               | NZE   |       |       | APC   |       |       | STEPS |       |       |
|-------------------------------------|---------------|-------|-------|-------|-------|-------|-------|-------|-------|-------|
| Water electrolyzer technology + PES |               | 2025  | 2030  | 2050  | 2025  | 2030  | 2050  | 2025  | 2030  | 2050  |
| AEM                                 | HYD           | 1.823 | 1.667 | 1.381 | 1.823 | 1.668 | 1.382 | 1.824 | 1.669 | 1.383 |
|                                     | WIND          | 2.011 | 1.798 | 1.420 | 1.999 | 1.794 | 1.420 | 1.988 | 1.786 | 1.423 |
|                                     | PV            | 3.476 | 2.608 | 1.667 | 3.357 | 2.694 | 1.706 | 3.515 | 2.703 | 1.732 |
|                                     | GRID          | 4.147 | 3.625 | 2.246 | 4.152 | 3.662 | 2.394 | 4.153 | 3.681 | 2.551 |
|                                     | HYD+WIND      | 1.917 | 1.733 | 1.400 | 1.911 | 1.731 | 1.401 | 1.906 | 1.727 | 1.403 |
|                                     | HYD+PV        | 2.649 | 2.138 | 1.524 | 2.680 | 2.181 | 1.544 | 2.669 | 2.186 | 1.558 |
|                                     | WIND+PV       | 2.744 | 2.203 | 1.543 | 2.768 | 2.224 | 1.563 | 2.751 | 2.244 | 1.577 |
|                                     | HYD+WIND+PV   | 2.437 | 2.025 | 1.489 | 2.453 | 2.052 | 1.503 | 2.442 | 2.052 | 1.513 |
|                                     | HYD+GRID      | 2.985 | 2.646 | 1.813 | 2.988 | 2.665 | 1.888 | 2.989 | 2.675 | 1.967 |
|                                     | WIND+GRID     | 3.079 | 2.712 | 1.833 | 3.076 | 2.728 | 1.907 | 3.071 | 2.733 | 1.987 |
|                                     | PV+GRID       | 3.811 | 3.117 | 1.956 | 3.845 | 3.178 | 2.050 | 3.834 | 3.192 | 2.142 |
|                                     | HYD+WIND+GRID | 2.660 | 2.364 | 1.682 | 2.658 | 2.375 | 1.732 | 2.655 | 2.378 | 1.786 |
|                                     | HYD+PV+GRID   | 3.149 | 2.633 | 1.764 | 3.171 | 2.675 | 1.827 | 3.164 | 2.684 | 1.889 |
|                                     | WIND+PV+GRID  | 3.211 | 2.677 | 1.777 | 3.229 | 2.717 | 1.840 | 3.219 | 2.723 | 1.902 |



Table B.13

Projected exergy costs of nitrogen via a cryogenic air separation unit based on the levelized exergy cost of electricity (LexCOE) for combinations of primary energy sources (PES) with grid under the IEA NZE, APC and STEPS energy transition scenarios [2,32,33] (Unit: kJ/kJ).

| N <sub>2</sub> exergy cost (kJ/kJ) | NZE    |        |        | APC    |        |        | STEPS  |        |        |
|------------------------------------|--------|--------|--------|--------|--------|--------|--------|--------|--------|
| Combination ASU + Grid             | 2025   | 2030   | 2050   | 2025   | 2030   | 2050   | 2025   | 2030   | 2050   |
| HYD                                | 7.199  | 7.173  | 7.092  | 7.200  | 7.175  | 7.097  | 7.201  | 7.178  | 7.103  |
| WIND                               | 7.946  | 7.739  | 7.291  | 7.898  | 7.718  | 7.294  | 7.853  | 7.682  | 7.307  |
| PV                                 | 13.758 | 11.234 | 8.562  | 14.002 | 11.603 | 8.763  | 13.911 | 11.640 | 8.898  |
| GRID                               | 16.421 | 15.621 | 11.539 | 16.440 | 15.781 | 12.301 | 16.527 | 15.862 | 13.111 |
| HYD+WIND                           | 7.573  | 7.456  | 7.192  | 7.549  | 7.446  | 7.195  | 7.527  | 7.430  | 7.206  |
| HYD+PV                             | 10.479 | 9.204  | 7.827  | 10.601 | 9.389  | 7.930  | 10.560 | 9.410  | 8.000  |
| WIND+PV                            | 10.852 | 9.486  | 7.927  | 10.950 | 8.661  | 8.030  | 10.882 | 9.661  | 8.102  |
| HYD+WIND+PV                        | 9.634  | 8.716  | 7.649  | 9.700  | 8.832  | 7.718  | 9.655  | 8.833  | 7.769  |
| HYD+GRID                           | 11.810 | 11.397 | 9.316  | 11.820 | 11.478 | 9.699  | 11.823 | 11.520 | 10.107 |
| WIND+GRID                          | 12.184 | 11.680 | 9.415  | 12.169 | 11.750 | 9.797  | 12.150 | 11.772 | 10.209 |
| PV+GRID                            | 15.090 | 13.427 | 10.051 | 15.221 | 13.692 | 10.532 | 15.179 | 13.751 | 11.004 |
| HYD+WIND+GRID                      | 10.522 | 10.178 | 8.641  | 10.513 | 10.225 | 8.897  | 10.500 | 10.240 | 9.174  |
| HYD+PV+GRID                        | 12.459 | 11.343 | 9.065  | 12.547 | 11.520 | 9.387  | 12.519 | 11.560 | 9.704  |
| WIND+PV+GRID                       | 12.708 | 11.531 | 9.131  | 12.780 | 11.701 | 9.452  | 12.737 | 11.728 | 9.772  |

## References

- G. Chehade, I. Dincer, Progress in green ammonia production as potential carbon-free fuel, *Fuel* 299 (2021) 120845.
- The Future of Hydrogen, International Energy Agency (IEA), 2019.
- Innovation Outlook: Renewable Ammonia, International Renewable Energy Agency (IRENA), Ammonia Energy Association (AEA), Abu Dhabi, Brooklyn, 2022.
- H. Ishaq, C. Crawford, Review and evaluation of sustainable ammonia production, storage and utilization, *Energy Convers. Manag.* 300 (2024) 117869.
- Sehkar, et al., A critical review of the state-of-the-art green ammonia production technologies- mechanism, advancement, challenges, and future potential, *Fuel* 358 (2024) 130307.
- T. Brown, Ammonia Energy Association, The capital intensity of small-scale green ammonia plants, 2018, URL: <https://www.ammoniaenergy.org/articles/the-capital-intensity-of-small-scale-ammonia-plants/>. (Accessed 19 February 2024).
- C. Smith, L. Torrente-Murciano, The importance of dynamic operation and renewable energy source on the economic feasibility of green ammonia, *Joule* 8 (1) (2024) 157–174, <http://dx.doi.org/10.1016/j.joule.2023.12.002>.
- Sun, et al., Modeling and simulation of dynamic characteristics of a green ammonia synthesis system, *Energy Convers. Manag.* 300 (2024) 117893.
- Wu, et al., Research on design and multi-frequency scheduling optimization method for flexible green ammonia system, *Energy Convers. Manag.* 300 (2024) 117976.
- Campion, et al., Techno-economic assessment of green ammonia production with different wind and solar potentials, *Renew. Sustain. Energy Rev.* 173 (2023) 113057.
- Resteli, et al., Detailed techno-economic assessment of ammonia as green H<sub>2</sub> carrier, *Int. J. Hydrog. Energy* 52 (2024) 532–547.
- M. Chatenet, et al., Water electrolysis: from textbook knowledge to the latest scientific strategies and industrial developments. In *Chemical society reviews* (vol. 51, issue 11, pp. 4583–4762), R. Soc. Chem. (2022) <http://dx.doi.org/10.1039/d0cs01079k>.
- S. Shiva Kumar, H. Lim, An overview of water electrolysis technologies for green hydrogen production, *Energy Rep.* 8 (2022) 13793–13813.
- X. Wei, et al., Comparative life cycle analysis of electrolyzer technologies for hydrogen production: Manufacturing and operations, *Joule* (2024) <http://dx.doi.org/10.1016/j.joule.2024.09.007>.
- A. Lima, J. Torrubia, A. Valero, A. Valero, Non-renewable and renewable exergy costs of water electrolysis in hydrogen production, *Energies* 18 (6) (2025) 1398, <http://dx.doi.org/10.3390/en18061398>.
- M. Penkuhn, G. Tsatsaronis, Comparison of different ammonia synthesis loop configurations with the aid of advanced exergy analysis, *Energy* 137 (2017) 854–864.
- D. Florez-Orrego, S. de Oliveira Junior, Modeling and optimization of an industrial ammonia synthesis unit: An exergy approach, *Energy* 137 (2017) 234–250.
- M.G. Gado, S. Nada, H. Hassan, 4E assessment of integrated photovoltaic/thermal-based adsorption-electrolyzer for cooling and green hydrogen production, *Process. Saf. Env. Prot.* 172 (2023) 604–620.
- Shamsi, et al., Evaluation of an environmentally-friendly poly-generation system driven by geothermal energy for green ammonia production, *Fuel* 365 (2024) 131037.
- G. Pagani, Y. Hajimolana, C. Acar, Green hydrogen for ammonia production – a case for the Netherlands, *Int. J. Hydrog. Energy* 52 (2024) 418–432.
- H. Ishaq, I. Dincer, Design and simulation of a new cascaded ammonia synthesis system driven by renewables, *Sustain. Energy Technol. Assess.* 40 (2020) 100725.
- Cao, et al., 4E analysis of ammonia production scenarios with different hydrogen production technologies, *Int. J. Hydrog. Energy* 102 (2025) 360–374, <http://dx.doi.org/10.1016/j.ijhydene.2025.01.005>.
- Koschwitz, et al., Exergoeconomic comparison of a novel to a conventional small-scale power-to-ammonia cycle, *Energy Rep.* 11 (2024) 1120–1134.
- Cameli, et al., Conceptual process design and technoeconomic analysis of an e-ammonia plant: Green H<sub>2</sub> and cryogenic air separation coupled with Haber-Bosch process, *Int. J. Hydrog. Energy* 49 (2024) 1416–1425.
- J. Torrubia, A. Valero, A. Valero, Non-renewable and renewable levelized exergy cost of electricity (lexcoe) with focus on its infrastructure: 1900–2050, *Energy* (2024).
- R. Pinto, et al., The rise and stall of world electricity efficiency: 1900–2017, results and insights for the renewables transition, *Energy* 269 (2023) <http://dx.doi.org/10.1016/j.energy.2023.126775>.
- A. Araújo, S. Skogestad, Control structure design for the ammonia synthesis process, *Comput. Chem. Eng.* 32 (12) (2008) 2920–2932, <http://dx.doi.org/10.1016/j.compchemeng.2008.03.001>.
- Szargut, et al., Exergy Analysis of Thermal, Chemical, and Metallurgical Processes, Hemisphere Publishing, New York, US, 1988, p. 350.
- C. Torres, A. Valero, The exergy cost theory revisited, *Energies* 14 (2021) 1594.
- C. Torres, A. Valero, A. Valero, TaesLab: An advanced software tool for circular thermoeconomics, in: *ECOS 2023: Efficiency, Costs, Optimization, Simulation, and Environmental Impact of Energy Systems*, 2023.
- J. Torrubia, et al., Energy and carbon footprint of metals through physical allocation. Implications for energy transition, *Resour. Conserv. Recycl.* 199 (2023) <http://dx.doi.org/10.1016/j.resconrec.2023.107281>.
- J. Torrubia, A. Lima, A. Valero, A. Valero, How renewable is green hydrogen? Analysis of the exergy cost of its production, in: *Proceedings ECOS 2024*, Rhodes, Greece, 2024.
- World Energy Outlook 2024, International Energy Agency (IEA), 2024.
- J. Torrubia, A. Valero, A. Valero, Renewable exergy return on investment (RExROI) in energy systems. The case of silicon photovoltaic panels, *Energy* (2024) 131961, <http://dx.doi.org/10.1016/j.energy.2024.131961>.
- IRENA, Green hydrogen cost reduction scaling up electrolyzers to meet the 1.5 °C climate goal, in: IRENA, 2020, [www.irena.org/publications](http://www.irena.org/publications).
- A. Lima, C. Torres, A. Valero, Circular thermoeconomics applied to a green ammonia synthesis plant: future production scenarios and alternative byproducts, in: *Proceedings ECOS 2024*, Rhodes, Greece, 2024.
- Carrasquer, et al., Exergy costs analysis of groundwater use and water transfers, *Energy Convers. Manage.* 110 (2016) 419–427, <http://dx.doi.org/10.1016/j.enconman.2015.12.022>.
- Net Zero Roadmap: A Global Pathway to Keep the 1.5 °C Goal in Reach - 2023 Update, International Energy Agency (IEA), 2023.
- M. Aneke, M. Wang, Potential for improving the energy efficiency of cryogenic air separation unit (ASU) using binary heat recovery cycles, *Appl. Therm. Eng.* 81 (2015) 223–231.
- A. Joint Research Centre, European Commission, Arrigoni, et al., Environmental life cycle assessment (LCA) comparison of hydrogen delivery options within Europe, in: European Commission, Joint Research Centre, 2024, <http://dx.doi.org/10.2760/5459>.
- Kakoulaki, et al., Green hydrogen in Europe – a regional assessment: Substituting existing production with electrolysis powered by renewables, *Energy Convers. Manag.* 228 (2021) 113649.
- International Trade and Green Hydrogen: Supporting the Global Transition to a Low-Carbon Economy, International Renewable Energy Agency (IRENA), World Trade Organization Agency (WTO), 2023.
- Sarker, et al., Prospect of green hydrogen generation from hybrid renewable energy sources: A review, *Energies* 16 (3) (2023) 1556.

- [44] H. Tao, et al., The gap between academic research on proton exchange membrane water electrolyzers and industrial demands, *Nature Nanotechnology* 19 (8) (2024) 1074–1076, <http://dx.doi.org/10.1038/s41565-024-01699-x>.
- [45] M. Laimon, S. Goh, Unlocking potential in renewable energy curtailment for green ammonia production, *Int. J. Hydrog. Energy* 71 (2024) 964–971, <http://dx.doi.org/10.1016/j.ijhydene.2024.05.022>.
- [46] D'Angelo, et al., Planetary boundaries analysis of low-carbon ammonia production routes, *ACS Sustain. Chem. Eng.* 9 (29) (2021) 9740–9749, <http://dx.doi.org/10.1021/acssuschemeng.1c01915>.
- [47] United Nations Environment Programme: Global Resources Outlook 2024: Bend the Trend – Pathways to a Liveable Planet as Resource use Spikes, United Nations (UN), Nairobi, 2024.
- [48] S. Vitta, Sustainability of hydrogen manufacturing: a review, *RSC Sustain.* 2 (11) (2024) 3202–3221, <http://dx.doi.org/10.1039/D4SU00420E>.
- [49] S. Mingolla, et al., Effects of emissions caps on the costs and feasibility of low-carbon hydrogen in the European ammonia industry, *Nat. Commun.* 15 (1) (2024) 3753, <http://dx.doi.org/10.1038/s41467-024-48145-z>.
- [50] R. Blay-Roger, et al., Natural hydrogen in the energy transition: Fundamentals, promise, and enigmas, *Renew. Sustain. Energy Rev.* 189 (2024) 113888, <http://dx.doi.org/10.1016/j.rser.2023.113888>.
- [51] N. Lefevvre, et al., Characterizing natural hydrogen occurrences in the Paris Basin from historical drilling records, *Geochem. Geophys. Geosyst.* 25 (5) (2024) <http://dx.doi.org/10.1029/2024GC011501>;  
S. Vitta, Sustainability of hydrogen manufacturing: a review, *RSC Sustain.* 2 (11) (2024) 3202–3221, <http://dx.doi.org/10.1039/D4SU00420E>.
- [52] N. Lefevvre, et al., Native H<sub>2</sub> exploration in the western Pyrenean foothills, 2021, <http://dx.doi.org/10.1002/essoar.10507102.1>.
- [53] M. Musa, et al., Techno-economic assessment of natural hydrogen produced from subsurface geologic accumulations, *Int. J. Hydrog. Energy* 93 (2024) 1283–1294, <http://dx.doi.org/10.1016/j.ijhydene.2024.11.009>.
- [54] G. Maroukis, M.C. Georgiadis, Modeling, simulation, and techno-economic optimization of argon separation processes, *Chem. Eng. Res. Des.* 184 (2022) 165–179, <http://dx.doi.org/10.1016/j.cherd.2022.06.003>.
- [55] M. Zhao, Y. Li, S. Sun, Analysis and optimization of two-column cryogenic process for argon recovery from hydrogen-depleted ammonia purge gas, *Chem. Eng. Res. Des.* 89 (7) (2011) 863–878.
- [56] Saedi, et al., Proposal and energy/exergy analysis of a novel cryogenic air separation configuration for the production of neon and argon, *Chem. Pap.* 76 (11) (2022) 7075–7093.
- [57] M. Yáñez, et al., PSA purification of waste hydrogen from ammonia plants to fuel cell grade, *Sep. Purif. Technol.* 240 (2020) <http://dx.doi.org/10.1016/j.seppur.2019.116334>.
- [58] T. Banaszkiewicz, M. Chorowski, Energy consumption of air-separation adsorption methods, *Entropy* 20 (2018) 232.
- [59] F. Eckl, et al., Valorization of the by-product oxygen from green hydrogen production: A review, *Appl. Energy* 378 (2025) <http://dx.doi.org/10.1016/j.apenergy.2024.124817>.
- [60] D. Tonelli, et al., Global land and water limits to electrolytic hydrogen production using wind and solar resources, *Nat. Commun.* 14 (1) (2024) 5532, <http://dx.doi.org/10.1038/s41467-023-41107-x>.
- [61] A. Valero, B. Palacino, S. Ascaso, A. Valero, Exergy assessment of topsoil fertility, *Ecol. Model.* 464 (2022) 109802.
- [62] S. Brynolf, M. Grahnl, Flexibility with low environmental impact, in: *Nature Energy*, 2024, <http://dx.doi.org/10.1038/s41560-024-01637-0>, *Nature Research*.
- [63] K. Dooley, et al., Over-reliance on land for carbon dioxide removal in net-zero climate pledges, *Nat. Commun.* 15 (1) (2024) <http://dx.doi.org/10.1038/s41467-024-53466-0>.